Response to reviews

'Dark-ice dynamics of the south-west Greenland ice sheet' by A. J. Tedstone *et al.*

Dear Prof. Tedesco,

We would like to thank both referees for taking the time to make detailed comments, which have resulted in a much-improved manuscript. We have taken care to add nuance to several sections of the manuscript. We respond inline to the referee comments below. Referee comments are in *italic* and changes in the manuscript are in **bold**.

We hope that you find our revisions make our manuscript suitable for publication in *The Cryosphere.*

Yours sincerely,

Andrew Tedstone, on behalf of the co-authors.

RC1

This is an informative study that combines remote sensing measurements of albedo with regional climate modeling to identify some of the factors that are associated with dynamics of the dark ice zone in southwest Greenland. The study does not offer any definitive conclusions about the actual processes governing these dynamics. But given that our understanding of biological controls on surface ice albedo is in its infancy, I think the associations between variables that are described here constitute a worthwhile contribution to the literature. The paper is quite well-written and includes insightful, if sometimes rather speculative, discussion.

The issues I describe below may require a bit of attention, though they are generally minor. I should add that a very similar remote sensing analysis was presented by Shimada et al (2016), and it seems important that the authors of that study should review and comment on this study. From my perspective, the present study seems to adequately describe its results within the context of Shimada et al. Furthermore, a novel component of the present study is that it combines regional climate simulations with the remote sensing analysis.

General issues:

The fact that the JJA melt-out-flux (MOF) is universally negative (Figure 4C) leads me to question the utility of this quantity. It is argued that when this quantity is positive conditions are favorable for melt-out of particles and unfavorable for cryoconite hole formation. But since the quantity is always negative during the summer, and since there is evidence (?) for melt-out of particles during summer, this quantity does not appear to be a good predictor of melt-out conditions. If this reasoning seems sound, I suggest that the authors consider removing this quantity altogether from the manuscript.

The cryoconite hole melt-out process was hypothesised as a driver of inter-annual variability in dark ice extent by Shimada et al (2016). The only evidence in the literature related to this hypothesis in the form of field measurements made in the south-west GrIS ablation zone by Chandler et al (2015)

(which we cite more extensively in the revised manuscript). These field measurements covered only a single season, 2015. Briefly, they presented limited evidence of cryoconite hole melt-out during a few days of warm, cloudy conditions, in which a few holes melted out but spatial coverage of cryoconite holes remained high. This event occurred in the context of an overall trend of increasing cryoconite hole coverage through the season. Hence, evidence for melt-out of cryoconite holes in summer is equivocal as the only field measurements from the GrIS to date show that melt-out does occur but not necessarily with widespread spatial impact.

We therefore tried to characterise the likelihood of cryoconite hole melt-out over wider spatial scales by defining the MOF quantity, which attempts to characterise 'warm, cloudy conditions' by considering the importance of sensible and longwave heat fluxes against shortwave fluxes. We note that we cannot test this experimental quantity (derived from a regional climate model) against field measurements as Chandler et al did not measure the full energy balance. We further assessed the potential for precipitation events to cause cryoconite hole melt-out, in case these events were not captured by MOF.

In summary, as existing evidence for the melt-out of cryoconite holes and associated climate conditions is equivocal, the MOF analysis is a key element of our analysis.

Sensible heat flux is deemed to be an important correlated variable with dark ice dynamics. How closely does the sensible heat flux track near-surface (or lower tropospheric) air temperature? They may be closely linked over Greenland. Sensible heat flux should loosely track (1) the difference in temperature between the air and surface, and (2) the near-surface wind speed. Since the ice surface is always at 0C when melting, the temperature difference is governed exclusively by air temperature. It is unclear, though, how important the wind speed is.

To examine this suggestion in further detail we use daily timeseries (average for the common area) of wind speed [UV], air temperature [TT], minimum air temperature [TTMIN] and sensible heat flux [SHF].

There is a strong correlation between TT and SHF (R^2 0.54, $p < 0.01$), and between TT and UV (R^2 0.67, $p < 0.01$). A multiple regression model of TT+UV~SHF also shows high correlation (R^2 0.80, $p < 0.01$). Imperfect correlations are to be expected given the averaging over the common area. This analysis indicates that both TT and UV are important in driving high SHF into the ice sheet surface.

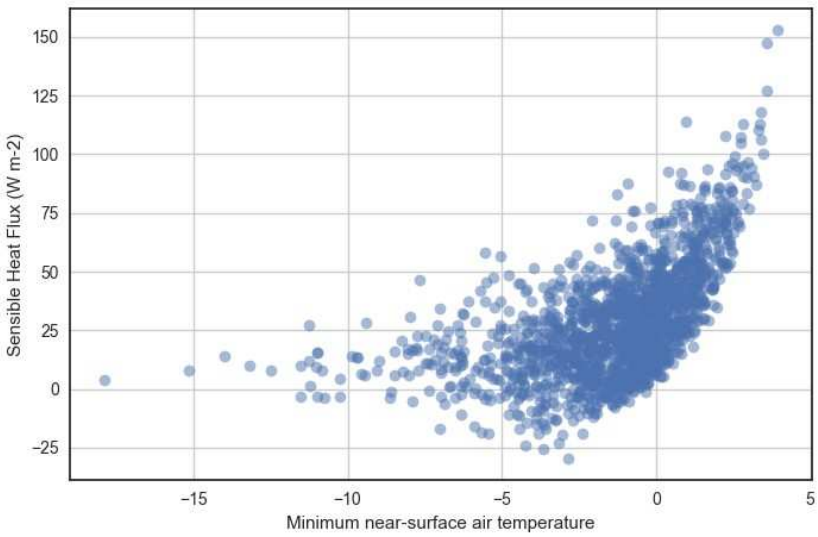

Response Figure 1. JJA minimum daily near-surface air temperature versus sensible heat flux, averaged over the common area. Both variables output by MAR.

However, we also note that, during JJA, positive daily TTMIN only occurs on days when SHF modelled at 12:00 is positive (Response Figure 1). We do not know the minimum daily SHF so cannot test for an association here, but nevertheless these results suggest a relationship between positive SHF and above-zero TTMIN.

Comparison of daily TTMIN and wind speed (Response Figure 2) suggests that, in general, positive TTMIN only occurs routinely at wind speeds in excess of ~6 m s^{-1}, which is also represented as a histogram in Response Figure 3. Thus, this suggests that higher wind speeds are the principal cause of higher SHF (i.e. into the ice sheet surface), and this higher SHF in turn makes positive TTMIN more likely.

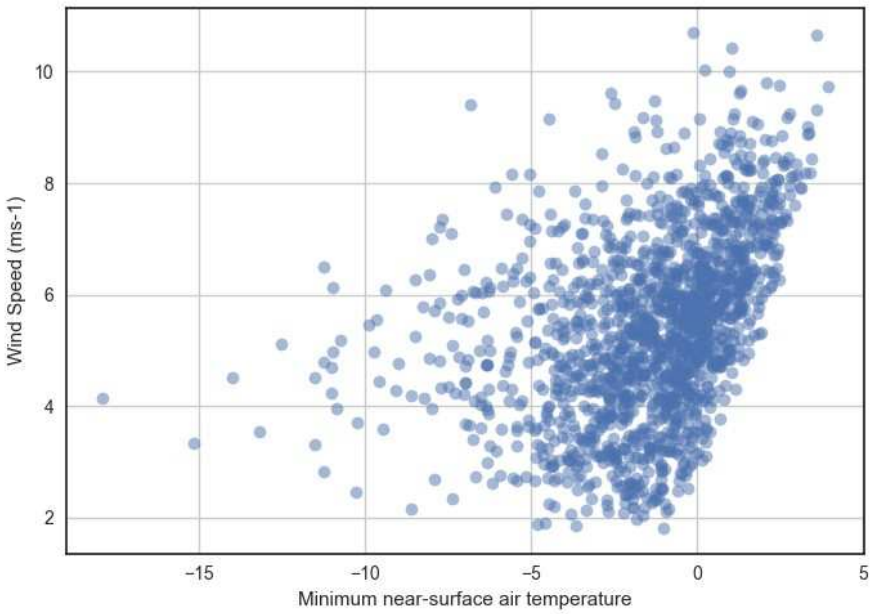

Response Figure 2. For JJA, daily minimum near-surface air temperature versus daily wind speed in the common area. Both variables output by MAR.

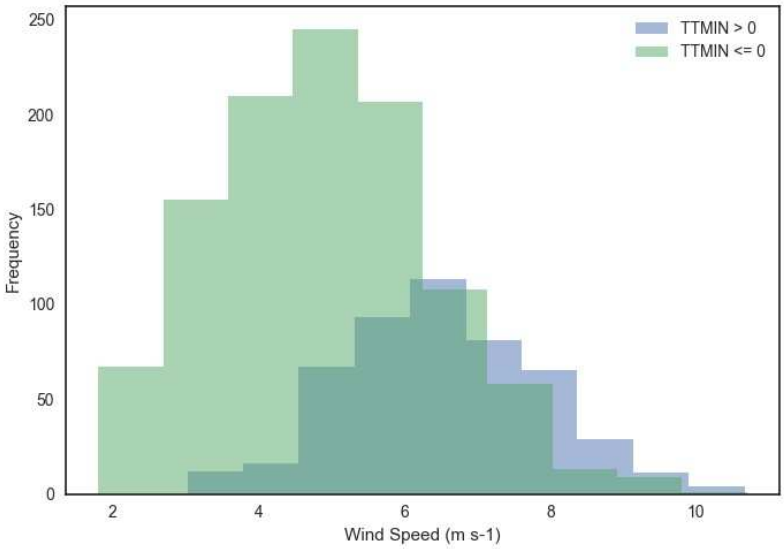

Response Figure 3. Histograms of daily wind speed in common area when the daily minimum temperature is below 0°C (green) compared to above 0°C (blue).

We have summarised these findings in the revised manuscript in **Sect. 3.2.2:**

> **Over daily timescales, higher SHF was associated with warmer near-surface air temperatures (R^2 0.54, $p < 0.01$) but more strongly with higher near-surface wind speeds (R^2 0.67, $p < 0.01$). Days on which the minimum air temperature was greater than 0 °C had mean wind speeds of 6.5 +-1.8 m s^{-1} +- 1 sigma), compared to 4.9 +- 1.3 m s^{-1} +- 1 sigma} on days when the minimum air temperature was 0 °C or less.**

And have noted in the Conclusions that **higher SHF was associated with higher wind speeds.**

The first paragraph of Data and Methods indicates that both MOD09GA and MOD10A1 MODIS reflectance/albedo products are used, but it is not clear to me which analyses and sections of the paper use which products. Please clarify this. Is MOD10A1 perhaps a derived product from MOD09GA, and it is really the former that is applied here? If so, please clarify this. Secondly, why is MOD10A1 used instead of other MODIS albedo product(s), like MCD43 for instance? Thirdly, please describe the native resolution of the MODIS data applied in this study.

MOD10A1 is a standalone product which is produced separately to MOD09GA. MOD10A1 is a daily albedo product, unlike MCD43 which is a multi-day composite product. In terms of our dark ice dynamics observations, the only part of the MOD10A1 product that we use is the cloud discrimination layer in order to mask our cloudy pixels in MOD09GA. However, we do use MOD10A1 albedo to compute SW_{net} as part of our MOF analysis (Sect. 2.5). The nominal resolution of MODIS sinusoidal gridded products is 500 m which we now note as follows:

> Both MODIS Level-2 products are delivered on a sinusoidal grid **at 500 m nominal resolution** which causes significant distortion…

p.4, line 29: "It is also noteworthy that R620-670nm straddles a transition zone between wavelengths mostly influenced by LAIs and wavelengths mostly influenced by grain evolution and interstitial water." - In that case, why is this wavelength chosen to discriminate dark ice (as darkened by LAIs), instead of a shorter wavelength?

620-670 nm is within the visible range and therefore predominantly affected by LAIs rather than grain evolution. Effects from grain evolution are likely minor at an upper bound of 670 nm; the statement noted above was partly due to an internal miscommunication, where the upper bound was accidentally thought to be ~700 nm.

Individual contaminants may alter the reflectance at specific wavelengths within the blue and green parts of the spectrum, compared to decreasing influence at longer visible wavelengths. For instance, heavy loading of certain dusts on snow can reduce the reflectance in the blue wavelengths but leave the green-red part of the spectrum reflecting efficiently (e.g. Skiles et al, 2017, *J. Glaciology*). As such, the red part of the spectrum is a better indicator of dark ice than the MODIS blue or green bands, which could lead to erroneous capture of dark snow as dark ice if the dust loading is high enough. We also note that our empirical evidence, in the form of field spectra presented in Appendix A, adequately show that thresholding 620-670 nm captures light and heavy algal blooms.

We have modified Sect. 2.1 to better reflect these factors:

> **However, we note that we do not know precisely what this dark ice threshold represents physically. The red band (620-670 nm) sits within the visible wavelengths and is therefore affected mostly by LAIs rather than grain evolution or water ponding, which mostly affect the near-infrared wavelengths (700-1100 nm). However, we caveat that other mechanisms can also reduce the reflectance across the entire solar spectrum, including in the red wave-band. These include reduction in volume-scattering due to wind or water 'polishing' the ice surface, infilling of interstitial air spaces with meltwater, and 'trapping' by roughness features such as crevasses. Nevertheless, by combining these thresholds we are able to distinguish at first order between clean and dark (LAI-laden) ice surfaces.**

The definition of intensity (D_I) given on p.5 is slightly unclear to me. Is D_I the average reflectance over the entire common area, or the average reflectance of the "dark" pixels within the common area? If it is the former, then D_I is affected both by the extent and the darkness of the dark ice, and it is therefore not independent of D_E. Please clarify this.

D_I is the average reflectance over the entire common area. We have clarified as follows:

> Third, intensity (D_I) was defined as the mean daily reflectance over 620-670 nm **of all cloud-free pixels in the common area**, and annual intensity as the mean of all cloud-free days in each JJA period.

The term "melt-out", as in "melt-out of particulates" is used frequently in this manuscript, but the precise meaning or process indicated by this term was at times unclear to me. I suggest clearly describing what is meant by "melt-out", at least at the first instance of its use.

In response to this comment we have **modified the manuscript so that the term 'melt-out' is used only in reference to the melt-out of cryoconite holes**. We no longer use this term when discussing ablating ancient ice as a source of particulates.

Minor comments:

p2, line 6: "Surface melting is controlled primarily by albedo" - I agree, but it would bolster your case to include one or more references in support of this claim.

Please see response to RC2.

p2, line 18: "The GrIS-wide bare-ice ablation zone extent increased by 4.4% per year..." - Is this a relative or absolute (as in percent of whole ice sheet) change? I assume the former, but please clarify.

On closely re-reading Shimada et al (2016) we find that it is neither option. Instead, the 4.4% per year is of the mean bare ice extent over 2000-2014. We have therefore rephrased as follows:

> The GrIS-wide bare-ice ablation zone extent increased by **7,158 km^2** per year on average from 2000 to 2014, although with substantial inter-annual variability of between 5 % **(89,975 km^2)** and 16 % **(279,075 km^2)** of the ice sheet **surface (Shimada et al., 2016)**.

p3, line 22: Is it necessary that the cryoconite reside beneath a layer of meltwater for the albedo increase to occur? Perhaps the melt layer augments the change, but I suspect the hole depth is the more important factor for hemispheric albedo increase. You might want to add nuance to this statement.

No it is not necessary, the reviewer is correct to suggest that the majority of the albedo increase is due to hiding the cryoconite at depth in the weathering crust; however, specular reflection from the water surface will enhance the effect by preventing incoming light from being 'trapped' by multiple reflection within the hole. We have edited the text as follows:

> Hole formation increases the albedo relative to dispersed cryoconite by sequestering the low-albedo cryoconite from the ice surface at depth, **resulting in a hemispheric albedo increase that will be further enhanced by specular reflection** when covered by a reflective layer of meltwater (Boggild et al, 2010).

p4, line 28: "precisely identify precisely"

Thank you, **corrected**.

p.5, line 18: "Only days in which at least 50% of the common area was cloud-free were included in the calculation" - And furthermore, were only cloud-free pixels used in this average? I assume so, but please clarify.

Correct, we have clarified as follows:

> Only days in which at least 50 % of the common area was cloud-free were included in the calculation, **and only the cloud-free pixels within the common area were used.**

p.6, line 4: "... equal-area 7.5 x 7.5 km..." - Earlier it is stated that model pixels are 600m x 600m. Please rectify this.

Our phrasing was confusing here. MODIS data are at 600 m, MAR at 7.5 km, but when we compare MODIS data with MAR outputs we bin MODIS data into MAR pixels:

> …yielding a spatial resolution of ~ 600 x 600 m. **When undertaking comparisons with MAR outputs, cloud-free MODIS data were binned into 7.5 km pixels to match MAR's resolution.**

Equation 4: It appears that SHF is defined as positive into the surface, but please confirm.

Yes, this is correct and **we now note this in Sect. 2.5** (Meteorological and climatological data).

p.7, line 13: "were been"

Thanks, **corrected.**

Figure 2 caption: "... the entire common area had D_I < 0.45." - Just to be sure, do you mean that every pixel in the common area had D_I < 0.45 (as communicated) or that the average D_I of the common area was less than 0.45?

Correct, caption updated:

> Black squares denote days on which the **average D_I of the cloud-free common area was < 0.45.**

Figure 2: What do the black triangles represent?

The black triangle represents the date of snow clearing $\tilde{t_B}$, as defined in the legend located in the upper-right of Figure 2. For clarity we have also added an explanation to the caption:

> **Black triangles denote the date of snow clearing, \tilde{t_B}.**

p.12, line 10: " ...The only published measurements of black carbon on the GrIS are from the north-west (Aoki et al, 2014; Polashenski et al, 2015)" - This statement needs refining, as there have been BC measurements from elsewhere on Greenland, including, e.g., by McConnell et al (2007, doi:10.1126/science.1144856) and Doherty et al (2013, doi:10.1002/jgrd.50235).

Thank you for drawing our attention to additional BC measurements in the literature. We have refined our statement to focus on surface (as opposed to ice-core) samples:

Measurements of black carbon **in snow on the present-day surface** of the GrIS **(as opposed to in ice cores)** have been made in the north-west (Aoki et al 2014, Polashenski et al 2015) **or high in the accumulation zone (Hegg et al 2010, Doherty et al 2013)**. However, at only a few ppb, these measurements of black carbon are insufficient to explain the substantial reduction in reflectance in the south-west (Shimada et al 2016).

p.13, line 2: missing citation

Apologies, a typo crept in at the last moment before submission, the citation is **Chandler et al. (2015, TC).**

p.14, line 23-25: Please see general comment about relationship between air temperature and SHF. I am wondering if the two quantities referenced in this sentence are closely related to each other. If so, it would be worth commenting on that here.

Please see our response to the associated general comment, above.

p.15, line 14: "... versus concentration of algae (D_I)..." - Related to my earlier comment, is D_I a true measure of algae concentration, or is it also affected by the extent of the dark zone?

D_I is purely a measure of how dark the entire common area is. The spatial extent of the common area is fixed for the entire duration of the study and so D_I is therefore independent of the extent of the dark zone. See also our response to earlier comment.

p.15, line 35: "across across"

Thank you, **corrected.**

In the figure captions, please describe the variables in addition to using their symbols.

We now describe the variables, or where the description would be excessively long, provide a reference back to where they are first defined.

<u>RC2</u>

Summary

MODIS satellite imagery is used to examine fluctuations in the extent of impurity-rich bare ice (dark ice) along the western margin of the Greenland Ice Sheet. A threshold on MODIS blue and red reflectance is used to identify bare ice and dark ice. Potential drivers of bare ice variability are examined using outputs of the MAR regional climate model, including shortwave radiation, longwave radiation, and sensible heat flux, in an attempt to understand causes of variability. The authors argue

that while outcropping particulates are a major factor in bare ice albedo variability, the presence of biological organisms may also play an important role.

General Comments

The topic covered by the paper is important to our understanding of factors contributing to fluctuations in the albedo of impurity-covered ice in the ablation area of the Greenland ice sheet. It overlaps somewhat with the recent study of Shimada et al. (2016), but extends the analysis to a full summer season and attempts to understand drivers of dark ice variability.

I feel the authors need better support for their arguments that biology is a major driver of bare ice albedo variability. There is no definitive proof for this and I don't think the authors have successfully ruled out melt-out of impurities, sub-grid scale variability in snow cover and/or superimposed ice, or even the presence of liquid water, as potential causes of the variability.

We are sympathetic to the concerns that referee 2 raises. At no point do we argue that we have definitive proof of '*biology*' constituting '*a major driver of bare ice albedo variability*'; the basis of this paper was rather to identify the most likely driving mechanisms of ice darkening. In conjunction with the existing literature our observations suggest that the most likely driving mechanism is biology, or, more specifically, algal growth. The referee goes on to discuss each of their other listed processes in more depth so please see our responses inline.

The authors have suggested that microorganisms appear to require the presence of outcropping material at the surface. If this is the case on a large scale, outcropping dust should control local and inter-annual variations in albedo as well. The authors' arguments that local-scale variability in dark ice extent can be explained not by dust melt-out, but by microorganisms, is inconsistent with the apparent need for dust as a microbial nutrient source on a larger scale.

We disagree. There is likely to be a significant difference between [A] the composition (not necessarily aborptive in visible spectrum) and concentration (relatively low) of outcropping materials required <u>as an input to algal growth</u>, for instance to supply nutrients, versus [B] the composition (absorptive in visible spectrum) and concentration (high) of outcropping materials necessary to <u>cause a reduction in surface reflectance</u> (e.g. Warren, 2013, *JGR*). The other pre-requisites of algal growth – meltwater presence and PAR – are then controlled by the meteorology of each melt season. Furthermore, we reiterate that we are unable to explain our temporal observations of dark ice dynamics by any known inorganic process (see discussion in Sect. 4.1), but that they do fit with darkening caused by the procession of algal growth.

Of course, over periods of several decades if outcropping dust is a fundamental pre-requisite to algal darkening then we would ultimately expect fluctuations in the dust supply rate to govern dark ice dynamics. However, our observations in this manuscript imply that over inter-annual timescales outcropping dust as a source of nutrients can be relied upon from one year to the next. Further examination of this topic is beyond the reach of our study, which is why we call for future field studies to quantify the distribution, mineralogy and ice-darkening potential of outcropping materials.

We have made various additions to the text, especially in Sect. 4.3, and also added some additional discussion to the end of Sect. 4.3 which draws on our response above.

See also our response to RC2 p.17 L 8-9.

I think that much of the variability the authors attribute to microorganisms could be attributed to dynamics of melt-out at small scales instead. Inter-annual variations in dark ice extent can be explained by the presence of superimposed ice, perhaps not fully accounted for in MAR. Increases in "Dark Ice Intensity" over time could be related to changes in surface cover within a relatively large MODIS grid box as snow patches and areas of superimposed ice melt away, exposing dark material beneath. The fact that sensible heat flux is a relatively important factor, as is the number of days where temperature is greater than zero suggests that melting of snow and ice could be an important factor independent of biological organisms. Therefore, there appears to be insufficient information to state definitively the cause of the variations in dark ice extent and intensity, although I think the authors have shown that local deposition from year to year can probably be ruled out as a contributing factor.

Given a lack of clear evidence supporting a biological source for inter-annual and intra-annual variability in bare ice albedo, I feel that the authors should reduce the emphasis on biological organisms as a source of variability and should also give credence to the possibilities mentioned above.

The authors should also address the possibility that the thresholds used here can falsely identify liquid water and possibility even snow or firn as ice or dark ice. The first is probably a minor factor, but the second could potentially lead to a misinterpretation of the results.

The work presented here provides a valuable investigation of variations in ice albedo and the presence of impurities in the ablation area of the Greenland ice sheet. I support publication of the study, provided the authors address the points provided in this review.

We think that there are two distinct issues here. The first concerns the seasonal transition of the surface from being snow-covered, through to firn by metamorphism, possibly a succession to reflective superimposed ice, and finally – assuming enough melting occurs – bare ice. The second concerns why bare ice may be 'dark' (or not) once snow has cleared.

Regarding delineation of snow and superimposed ice from bare/dark ice: as stated in the Methods, we take care to first delineate bare ice from snow-covered surfaces using MODIS band 2 (841-876 nm), which is sensitive to the snow/ice transition via grain size. We therefore do not rely on MAR for this part of the analysis like the comment implies. Only once MODIS observations indicate a pixel is clear of snow do we apply the dark ice threshold to MODIS band 1 (620-670 nm).

Regarding the importance of snow and superimposed ice on dark ice dynamics: it is well known that ablation rates in this sector of the ice sheet are high, on the order of metres per year (e.g. Sole et al., 2013, *GRL*; van As et al., 2016, *GEUS Bulletin*), and so ablating bare ice is usually exposed for much of the melt season. It is therefore hard to envisage a situation in which superimposed ice layers have more than a transient impact upon dark ice intensity, and indeed also to envisage how the small-scale dynamics of snow patches melting could drive regional dark ice dynamics for the entire melt season. Our **addition of the inter-quartile range of bare ice appearance derived from MODIS to Figs 2 and 3** indicates that snow generally clears over a relatively short period near the start of the season (although we acknowledge that sub-pixel patches of snow may still remain).

Furthermore, our observations show that dark ice, as distinct from bare ice is not a static nor omnipresent layer lying beneath snow or superimposed ice. In turn, this suggests that some set of

processes is at work which allows dark ice duration, extent and intensity to vary both through a single melt season after the snow has cleared and between successive melt seasons.

Regarding the comment '*The fact that sensible heat flux is a relatively important factor...suggests that melting of snow and ice could be an important factor independent of biological organisms*', we also examined the relationship between the SHF anomaly (relative to 1981-2010 JJA climatology) and D_N for only the period between snow retreat (as identified by MODIS band 2) and the end of August each year, as opposed to over the entire JJA period. We did not include this analysis in our original manuscript for reasons of space and clarity. The R^2 for this relationship is 0.40, almost the same as for JJA SHF (0.41, Figure 5e). We therefore conclude that SHF has an important relationship with bare-ice darkening even after the snow has cleared.

Regarding mixed reflectance: the reflectance threshold we use to delineate dark ice is conservative and field-derived, based on a surface loaded with light algae as compared to a bare ice surface (Appendix A). We apply this threshold – acquired from patches on the order of 20 cm in diameter – to the reflectance value captured for entire MODIS pixels at 600 x 600 m.

The reviewer is correct that there is still potential for mixed reflectance within a MODIS pixel, due for instance to snow patches and superimposed ice, to impact on dark ice intensity values. We already caveat in Sect. 4.3 that we are unable to examine the subpixel extent of dark ice. Considering our field-validated thresholds, the presence of snow/superimposed ice is likely to be more important for pixel-wide dark ice intensity > ~ 0.45, and so we take care in Figure 2 to label the days on which the entire cloud-free extent of the common area has a dark ice intensity < 0.45. For the common area intensity to be < 0.45 but still influenced by high-reflectance snow and/or superimposed ice then there would also need to be widespread 'heavy algae' (Appendix A) in order to pull the area-averaged reflectance down enough to pass the dark ice threshold, which we suggest is unlikely.

More broadly, we have tried to take care to caveat that snow patches and areas of superimposed ice will have an impact on dark ice intensity, especially early in the melt season. As we noted in the manuscript (Sect. 4.3, para. 3), Chandler et al. (2015) reported the presence of a reflective surface immediately after snow clearing, which they attributed to a layer of superimposed ice. But on longer time-scales this is very likely to melt away revealing (as the reviewer notes) 'dark material beneath'. The sensible heat flux is likely to constitute an indirect influence on bare-ice algal assemblages through direct snow (and superimposed ice) removal – which we have already argued in discussion P14, Line 26 onwards.

Following on from our responses above and to the previous general comment, **we have made several small additions to our existing caveats in Sect 4.3, especially para 4 – see manuscript for details.**

Specific Comments

P. 1, Line 1: The recent increases in runoff are not caused by reduced albedo but by changes in atmospheric circulation and atmospheric warming. Albedo changes resulting from these changes amplify melt. Please clarify.

Thanks for spotting this mistake. Clarified:

> Runoff from the Greenland Ice Sheet (GrIS) has increased in recent years due largely to **changes in atmospheric circulation and atmospheric warming. Albedo reductions resulting from these changes have amplified surface melting.**

P. 1, Line 7: Add "in the future" after "will evolve".

Done.

P. 2, Line 6: The statement that "surface melting is controlled by albedo" should be clarified. Other components of the energy balance certainly play a role in controlling melting. Albedo can only play a role with sufficient downward shortwave radiation. Melting can potentially occur during portions of the year when there is less solar radiation as a result of sensible, or longwave fluxes. Please revise this statement, e.g. "Surface albedo plays an important role in modulating surface melt as the surface darkens with warming temperatures…."

Thanks, we have rephrased following your suggestion:

> Surface albedo **plays an important role in modulating the surface melt caused by incoming shortwave radiation.**

P. 3, Line 34 – P. 4, Line 4: Is there a reference to which the authors can refer here or are these unpublished results of the authors? Please clarify the source in the text.

Apologies, there was a reference missing here – **ref to Lutz et al (2014) inserted**, who undertook opposed pyranometer measurements.

P. 4, Line 8: Independent of these processes, there is also the possibility of consolidation of impurities at the surface due to melt, which the authors do discuss later in the manuscript. Perhaps change "inorganic particulate deposition" to "inorganic particulate deposition or redistribution".

Done.

P. 4, Lines 28-29: These are all good points, but perhaps now say what the authors think can be done using the thresholds used here.

Combining the 0.84 and 0.67 um thresholds we can identify bare ice and then distinguish between bare ice that is clean, and bare ice that is significantly darkened by LAI's - which we define as 'dark ice'. This is a significant capability in itself as it enables the mapping of dark ice that needs to be explained. **See also our response to RC1, p.4, line 29, which resulted in changes to this section.**

P. 4, Lines 29-30: Are the authors saying that some of the variability in extent or intensity could then be associated with grain size evolution and the presence of water? Please clarify.

Please see our response to RC1, P.4, L29-30, **which resulted in changes to this section.**

P. 5, Line 1: Clarify how the maximum area was defined, e.g. using daily MODIS reflectance values.

We already explain how the maximum area is defined in P.5, lines 6-9.

P. 5, Line 8: Explain why pixels 1 km from the ice sheet margin were removed.

Pixels near the ice sheet margin can be a mixture of land and ice, and thus are likely to exhibit low reflectance whether or not the ice is dark. To handle locations where the ice mask used here does not precisely match the 600 m resolution of our MODIS data we minimize this 'false positive' by only keeping pixels > 1 km from the margin. We have changed the manuscript as follows:

> Finally, we removed all dark pixels which occurred within ~1 km of the ice sheet margin as **defined by the Greenland Ice Mapping Project (GIMP; Howat et al 2014) in order to remove errant pixels consisting of mixed land and ice cover which remained after applying the GIMP ice area mask.**

P. 5, Lines 11-12: What is meant by "all the pixels", the number of pixels or fraction of pixels?

Rephrased:

> First, annual extent (D_E) corresponds to the extent **(in km^2) covered by the pixels** within the common area which were dark for at least 5 d in each year.

P. 5, Line 13: Clarify that this is the percentage of all daily cloud-free observations that were classified as "dark" in each JJA period.

Rephrased:

> Second, annual duration (D_D) was defined at each pixel in the common area as the percentage of daily cloud-free observations made in each JJA period **which were classified as dark**, and is thereby normalised for cloud cover.

P. 5, Line 15-16: It is a bit confusing to refer to this as intensity and to have a lower number indicate a larger intensity. Can't this just be referred to as the average reflectance? Then a lower reflectance is associated with a darker surface.

Yes it could be in principle. This is a matter of styling preference - we chose D_I in order to correspond with the other dark ice metrics.

P. 6, Line 6: Include a reference for the ECMWF reanalysis: (Dee et al., 2011) doi:10.1002/qj.828

Done.

P. 6, Line 15: Is the daily energy for melt-out "MOF"? Define MOF here. Based on the authors statements it doesn't seem that the MOF is necessarily a proven measure of the conditions needed to produce melt-out. If so it should be made clear that the MOF is suggestive of the conditions needed to cause melt-out, but does not necessarily indicate whether melt-out is occurring or not.

Yes, the referee is correct that the MOF is not a proven measure of melt-out conditions.We have made the following changes:

> Sect. 2.5: **We therefore characterised the conditions which could cause melt-out of cryoconite holes as the `melt-out flux', MOF**, using... [equation]
>
> Sect. 3.2.2: We examined the likelihood for cryoconite hole melt-out (causing redistribution of cryoconite materials onto the ice sheet surface) using MOF (Fig. 4c) **which is suggestive of the energy balance conditions that are needed to melt cryoconite holes out of their weathering crust.**

Our response to referee 1 on the topic of MOF is also relevant.

P. 7, Line 4: Clarify that this "extension is relative to the study of Shimada et al. (2016), which only examined July.

Done.

P. 7, Line 8: Change "time lag…" to "time lag between tB and the first identified occurrence of dark ice of 10-15 days".

Done.

P. 7, Line 10: Anticyclonic days don't seem to be shaded gray in Fig. 4.

We assume the referee means to refer to Fig. 2. Our version of the figure clearly shows the cloudy days in gray; we request that the TC typesetting office confirm this prior to final publication.

P. 9, Line 6: Change "magnitude of dark ice" to something like "extent and intensity of dark ice" or "extent and reflectivity of dark ice".

Changed to '**extent and intensity** of dark ice'.

P. 9, Line 8: Clarify "years when the ice went dark". Perhaps "years when DE was higher" would be more specific.

We agree – **changed as suggested.**

P. 9, Line 22: Change "Not only was winter snowfall" to "Not only was 2014-2015 winter snowfall…" for clarity.

Changed.

P. 11, Line 24: Briefly note how the weathering crust forms.

Revised, **now notes the importance of subsurface melt by incoming shortwave radiation** (c.f. Cook et al, 2016, Hydro. Proc.).

P. 12, Line 27: Should "decimeter" be "decameter"?

Correct, thanks for spotting – **changed.**

P. 12, Line 21 – P. 13 Line 2: I am not totally convinced by this argument. Much of this could be explained by the presence of superimposed ice, sub-grid scale exposure of bare ice, or even the presence of firn that is mis-classified as bare ice. I don't think the authors can rule out melting as a primary cause of the observed variability, especially since they do not utilize measurements or estimates of melt here. I think the authors should be more careful to acknowledge that melt could be responsible for the observed variability, but that the results also suggest that other factors could be involved.

Please see our response to the general comment from RC2, above.

P. 13, Lines 17-25: The variability the authors are discussing seems consistent with the hypothesis of Shimada et al. (2016) except with regard to the changes in dark ice intensity during 2012 and between 2012 and 2013. The statement that "our results reveal a different spatio-temporal pattern" is therefore a bit confusing. As for previous section, the changes in intensity during 2012 could be explained by sub MODIS-grid-scale processes such as melting of snow patches, collecting meltwater. 2012 was a high melt year while 2013 was a low melt year. During 2013, ice is exposed for a much shorter length of time, and the presence of superimposed ice, or again, patches of snow covering the ice could explain the lack of dark ice during that year.

We note firstly that while stating that our results are 'consistent' with Shimada et al, this comment does not acknowledge the dark ice dynamics of 2011 and 2012, which was the crux of our discussion and of Shimada et al's argument in favour of cryoconite hole processes. We reiterate that our observations of dark ice dynamics do not support cryoconite hole processes as the source of dark ice variability once the full JJA periods of 2011 and 2012 are taken into account; full details are in the manuscript.

Much of our response to this referee's general comment about *the impact of snow patches and superimposed ice* is relevant to the questioning here of dark ice dynamics during 2012 compared to 2013. In addition, we note that 2012 was the highest melt year on record, and so whilst sub-pixel variability in snow and/or super-imposed ice may have been transiently important to the darkening signal during the start of the melt season in early June, it is highly unlikely that they would have

continued to have an impact on dark ice metrics in July and August. See, for example, Tedstone et al. (2013, *PNAS*), which showed that positive degree days were experienced on almost every single day in this area all the way up to ~1450 m asl until late August.

For 2013, we acknowledge that the melt season was so short that it is possible that snow patches/superimposed ice could have had an impact on dark ice metrics despite MODIS band 2 indicating that the snow had cleared. We now caveat the 2013 statement by saying that prolonged presence of snow patches and/or superimposed ice could have limited dark ice extent:

> This also makes it difficult to explain low D_E in 2013, as cryoconite holes would have needed to form over a short period at the end of summer 2012 in order to sequester cryoconite particles at depth, unless the presence of snow patches and/or superimposed ice at the surface was so prolonged that only in a few pixels did enough melting take place to expose bare/dark ice.

We also note that we have added the inter-quartile range of bare ice appearance date to Figures 2 and 3.

P. 17, Lines 8-9: The surface must be a mixture of impurities and biological materials, or could even be abiotic. How is the material assumed to be algae?

The material is indeed a mixture of algal and abiotic impurities; however, microscopic examination showed very clearly that the majority of the impurity load comprised dark coloured algal cells with a relatively very low concentration of mostly clear quartz dust particles. An example of such an example may be found in Yallop et al. (2012, *ISME*). Even by eye, the surface is clearly discoloured mainly by a film of organic matter rather than dust granules which was confirmed to be pigmented algae using a field microscope. **We have added a summary of this information to Appendix A.** Detailed analysis of the constituents will be presented in further papers.

Figure 1: It would be useful for the reader to include numbers indicating the value of DE for each image.

Done.

Figure 2: Mention tB in the caption.

Done.

Figure 3: Note that the snow depth is from MAR. It would be interesting to also see tB in this figure, to allow for a comparison with MAR.

We have added ~t_B. We have also added the inter-quartile range of the date of bare ice appearance each year as determined from MODIS to both figures 2 and 3.

Technical Corrections

P. 4, Line 15: Change "cloud" to "clouds".

Done.

P. 4, Line 28: Change "precisely identify precisely" to "precisely identify"

Done.

P. 5, Line 18: Add "(DN)" after "normalized darkness" for clarity.

Done.

P. 5, Line 27: The phrase "with any…only allowed to be cloudy" is confusing. Perhaps just change to "excluding cloudy days".

Apologies, this interpretation is not correct. Aiming to prevent further confusions we have therefore rephrased as follows:

> Each year, we identified the first rolling window at each pixel that contained at least 3 days of bare or dark ice (not necessarily consecutive) **and 0 days of non-bare or non-dark ice, which therefore permitted up to 4 days of cloud cover in the window.**

P. 6, Line 12: Place a parenthesis around (T>0) for clarity.

Done.

P. 7, Line 13: Change "were been" to "were"

Done.

P. 9, Line 3: Change "not explicable by" to "cannot be explained by"

Done.

P. 9, Line 14: Change "snowfall which occurs" to "snowfall that occurs"

Done.

Dark ice dynamics of the south-west Greenland Ice Sheet

Andrew J. Tedstone[1], Jonathan L. Bamber[1], Joseph M. Cook[2], Christopher J. Williamson[1], Xavier Fettweis[3], Andrew J. Hodson[2], and Martyn Tranter[1]

[1]Bristol Glaciology Centre, School of Geographical Sciences, University of Bristol, Bristol, UK
[2]Department of Geography, University of Sheffield, Winter Street, Sheffield, UK
[3]Laboratory of Climatology, Department of Geography, University of Liège, Liège, Belgium

Correspondence to: Andrew Tedstone (a.j.tedstone@bristol.ac.uk)

Abstract. Runoff from the Greenland Ice Sheet (GrIS) has increased in recent years due largely to ~~declining albedo and enhanced~~ changes in atmospheric circulation and atmospheric warming. Albedo reductions resulting from these changes have amplified surface melting. Some of the largest declines in GrIS albedo have occurred in the ablation zone of the south-west sector and are associated with the development of 'dark' ice surfaces. Field observations at local scales reveal that a variety of light-absorbing impurities (LAIs) can be present on the surface, ranging from inorganic particulates, to cryoconite materials and ice algae. Meanwhile, satellite observations show that the areal extent of dark ice has varied significantly between recent successive melt seasons. However, the processes that drive such large inter-annual variability in dark ice extent remain essentially unconstrained. At present we are therefore unable to project how the albedo of bare-ice sectors of the GrIS will evolve in the future, causing uncertainty in the projected sea level contribution from the GrIS over the coming decades.

Here we use MODIS satellite imagery to examine dark ice dynamics on the south-west GrIS each year from 2000 to 2016. We quantify dark ice in terms of its annual extent, duration, intensity and timing of first appearance. Not only does dark ice extent vary significantly between years, but so too does its duration (from 0 % to > 80 % of June-July-August, JJA), intensity and the timing of its first appearance. Comparison of dark ice dynamics with potential meteorological drivers from the regional climate model MAR reveals that the JJA sensible heat flux, the number of positive minimum-air-temperature days and the timing of bare ice appearance are significant inter-annual synoptic controls.

We use these findings to identify the surface processes which are most likely to explain recent dark ice dynamics. We suggest that whilst the spatial distribution of dark ice is best explained by outcropping of particulates from ablating ice, these particulates alone do not drive dark ice dynamics. Instead, they may enable the growth of pigmented ice algal assemblages which cause visible surface darkening, but only when the climatological pre-requisites of liquid meltwater presence and sufficient photosynthetically-active radiation fluxes are met. Further field studies are required to fully constrain the processes by which ice algae growth proceeds and the apparent dependency of algae growth on melt-out particulates.

1 Introduction

Overall mass losses from the Greenland Ice Sheet (GrIS) have increased substantially since the early 1990s (Rignot and Kanagaratnam, 2006; Rignot et al., 2011; Shepherd et al., 2012). The average rate of mass loss increased from 34 $\mathrm{Gt\ yr^{-1}}$

during 1992–2001 to 215 $\mathrm{Gt\ yr^{-1}}$ during 2002–2011 (Sasgen et al., 2012). During 1991-2015 the GrIS lost mass at a rate equivalent to approximately $0.47 \pm 0.23\ \mathrm{mm\ yr^{-1}}$ of sea level rise, with a peak contribution in 2012 of 1.2 mm (van den Broeke et al., 2016). Increases in mass losses since 2009 have been dominated by increased surface runoff, with only 32 $\%$ of the total loss in this period attributable to solid ice discharge (Enderlin et al., 2014). It is therefore essential to understand the processes which control surface melting in order to be able to quantify the contribution of the GrIS to sea level rise over the coming century.

Surface ~~melting is controlled primarily by albedo~~ albedo plays an important role in modulating the surface melt caused by incoming shortwave radiation. A lower albedo permits more absorption of shortwave radiation, which in turn leads to enhanced ice melting, and so albedo is the dominant factor governing surface melt variability in the ablation area (Box et al., 2012). The effective albedo of the GrIS is controlled by external factors including solar zenith angle, atmospheric composition and cloud cover, as well as the inherent optical properties of the surface. For both snow-covered and bare-ice surfaces these inherent optical properties are modified by (a) ice grain metamorphism, (b) meltwater on the surface or in interstitial pores, and (c) light-absorbing impurities (LAIs) including biological and mineralogical substances (Gardner and Sharp, 2010), each of which generally lead to reduced albedo.

Declines in GrIS bare-ice albedo have an immediate impact on runoff from the GrIS and hence the surface mass balance (SMB). Decreases in the SMB since 1991 are predominantly due to enhanced runoff from bare-ice, low-lying (<2000 $\mathrm{m.a.s.l.}$) parts of the ice sheet (van den Broeke et al., 2016). Since around 2000 the surface albedo of several sectors of the GrIS has often been significantly lower each summer than was observed during the 1990s (He et al., 2013). GrIS summer albedo showed a negative trend during 2000-2012, with the largest decreases observed in western Greenland (Stroeve et al., 2013). Some of the decline in albedo can be attributed to increases in bare-ice extent. The GrIS-wide bare-ice ablation zone extent increased by ~~4.4~~ 7,158 $\mathrm{km^2}$ per year on average from 2000 to 2014, although with substantial inter-annual variability of between 5 $\%$ (89,975 $\mathrm{km^2}$) and 16 $\%$ (279,075 $\mathrm{km^2}$) of the ice sheet surface (Shimada et al., 2016).

In the ablation zone of the south-west GrIS, albedo lowered by as much as 18% from 2000 to 2011 (Box et al., 2012). The south-west has seen the greatest increase in bare-ice extent, by on average 5.8 $\%$ per year, with a mean extent of 56,603 $\mathrm{km^2}$ during 2000–2014 (Shimada et al., 2016). However, increasing bare-ice extent alone is insufficient to explain the declining albedo. Remotely-sensed optical imagery for this sector shows a band of relatively darker ice within the bare-ice ablation zone which recurred annually in the same location over the period 2001–2007, beginning 20–30 km inland from the ice sheet margin and extending up to $\sim$50 km wide, which has been postulated to be caused by LAIs (Wientjes and Oerlemans, 2010). LAIs on snow/ice surfaces reduce reflectance the most in the visible part of the solar spectrum (Warren, 1984; Painter et al., 2001; Bøggild et al., 2010), and this effect enabled Shimada et al. (2016) to quantify the inter-annual extent of dark ice — both GrIS-wide and for the south-west sector — by applying an empirically-derived reflectance threshold to the 620-670 nm band of MODIS satellite imagery acquired in July each year. They found that dark ice extent varied substantially between years, both GrIS-wide (from 3575 to 26,975 $\mathrm{km^2}$) and in the south-west (from 575 to 15,025 $\mathrm{km^2}$).

There are a range of possible causes of dark ice on the GrIS. One ~~is the melt-out of particulates from~~ consists of outcropping particulates in ablating ice. Wientjes et al. (2012) acquired shallow ice cores from the south-west sector in which they found

dust that they dated to the Late Holocene. They therefore suggested that the dust was deposited in the accumulation zone and flowed with the ice down to the ablation zone~~where it has been melting out in recent years~~, causing darkening of the surface as the ancient ice melts. However, they were not able to measure absolute concentrations of dust in their ice cores to compare to non-dark regions of the ice sheet. Meanwhile, Shimada et al. (2016) found a statistically significant correlation (r = 0.69) between July dark ice extent and air temperature (and hence surface melt rates, potentially ~~causing enhanced particulate melt-out~~depositing more particles from the ancient ice on the surface) in the south-west sector, but did not identify the responsible component of the surface energy balance.

Another potential source of darkening is the deposition of black carbon and other inorganic impurities by wet and dry atmospheric deposition, which has been investigated in ice and snow elsewhere (Warren and Wiscombe, 1980; Warren, 1984; Warren and Wiscombe, 1985; Gardner and Sharp, 2010). However, black carbon appears unlikely to explain variations in dark ice on the south-west GrIS. First, concentrations of black carbon in snowpack in the north-western snow sector are too low to cause any appreciable darkening and have been stable or even slightly declining over the past decade (Polashenski et al., 2015). Second, fire events in North America and Eurasia became rarer from 2002 to 2012 (Tedesco et al., 2016). Third, there is no recent statistically significant trend in aerosol flux deposition estimates along the south-west margin of the ice sheet (Tedesco et al., 2016).

In addition to inorganic impurities alone, the ice sheet can be darkened by ice surface habitats. Cryoconite is an aggregate of inorganic materials bound together by extracellular polymers produced by microorganisms, predominantly cyanobacteria (Wharton et al., 1985; Takeuchi et al., 2001; Hodson et al., 2008; Cook et al., 2016a). Cryoconite absorbs more shortwave radiation than the surrounding ice and so, when the surface energy balance is dominated by shortwave radiation, ice overlain by cryoconite will melt more quickly than the surrounding ice. This produces water-filled cryoconite holes with a floor of biologically-active sediment (Gribbon, 1979; Cook et al., 2016a). These holes range from a few centimetres to several metres in diameter and depth (MacDonell and Fitzsimons, 2008), can cover a large part of the ablation zone (Hodson et al., 2008), and have been observed to occur in the south-west region of the GrIS (Stibal et al., 2012; Cook et al., 2012; Chandler et al., 2015; Stibal et al., 2015; Cameron et al., 2016). Hole formation increases the albedo relative to dispersed cryoconite by sequestering the low-albedo cryoconite from the ice surface at depth~~beneath~~, resulting in a hemispheric albedo increase that will be further enhanced by specular reflection when covered by a reflective layer of meltwater (Bøggild et al., 2010). Occasional stripping events ~~cause redistribution of aggregates onto~~ associated with high ambient air temperatures have been observed in the McMurdo Dry Valleys, Antarctica, resulting in cryoconite hole melt-out, the redistribution of cryoconite aggregates over the ice surface and subsequent ~~new hole formation (MacDonell and Fitzsimons, 2008; Irvine-Fynn et al., 2011)~~ formation of new holes (MacDonell and Fitzsimons, 2008) . Similarly, in the south-west ablation zone of the GrIS, Chandler et al. (2015) observed that in warm, cloudy conditions some cryoconite holes melted out and release debris, but with little corresponding reduction in cryoconite hole coverage, and set against an overall increasing trend in cryoconite hole coverage as the 2015 melt season progressed.

Distinct from the assemblages of microorganisms associated with cryoconite holes, ice algae can bloom in the upper few centimetres of bare melting ice. Abundant assemblages of ice algal communities have been reported on bare ice in both west

(Uetake et al., 2010; Yallop et al., 2012) and east Greenland (Lutz et al., 2014). Ice algae produce specialist pigments which absorb UV and visible wavelengths, protecting the photosynthetic apparatus from excessive radiation (Dieser et al., 2010; Yallop et al., 2012; Remias et al., 2012). These pigments may be a significant source of darkening to GrIS surface ice (Yallop et al., 2012; Lutz et al., 2014).

The influence of cryoconite, cryoconite hole processes, and/or ice algal assemblages on the substantial inter-annual variability apparent in dark ice extent of the GrIS is currently unknown. Whilst Shimada et al. (2016) proposed cryoconite sequestration into cryoconite holes as the mechanism underlying the negative correlation (r = -0.52) between ice-sheet-wide July dark ice extent and shortwave radiation, this relationship did not hold when examined for the south-west sector alone. Additionally, although opposed pyranometer measurements (300–1100 nm) demonstrated that local algal bloom patches on snow had lower albedo at these wavelengths than snow without visible blooms (Lutz et al., 2014), broadband albedo measurements relevant for energy balance have not been isolated from grain evolution, meltwater ponding and abiotic impurities.

In this study we aim to identify the 'top-down' controls of significant variability in dark ice extent between successive melt seasons in the south-west of the GrIS. We first characterise the inter-annual dark ice dynamics of the south-west GrIS using visible satellite imagery to quantify dark ice in terms of its extent, duration, intensity and the timing of its appearance each year. We then examine the extent to which inter-annual variations in dark ice dynamics are controlled by prevailing seasonal meteorological and climatological conditions and how they could drive surface darkening through three potential processes: (1) inorganic particulate deposition or redistribution, (2) cryoconite hole processes and (3) growth of ice algal assemblages.

2 Data and Methods

2.1 Identification of dark ice

We used the MOD09GA Daily Land Surface Reflectance Collection 6 product, which is derived from data acquired by the MODIS sensor on board NASA's Terra satellite, to map bare and dark ice. Collection 6 products include improved calibration algorithms to correct for MODIS sensor degradation on Terra (Lyapustin et al., 2014) which was responsible for an apparent decline in GrIS dry snow albedo over the last decade or so (Polashenski et al., 2015; Casey et al., 2017). We used the clouds discrimination layer of the MOD10A1 Daily Snow Albedo Collection 6 product ~~, which contains a cloud discrimination layer,~~ to identify and discard pixels covered by cloud. Our full time series encompasses daily observations between May and September from 2000 to 2016 but here we concentrate mainly on observations made during JJA.

Both MODIS Level-2 products are delivered on a sinusoidal grid ~~which causes~~ at 500 m nominal resolution which exhibits significant distortion over the GrIS and prevents simple comparison with meteorological fields output by the regional climate model MAR (Sect. 2.5). We therefore first re-projected the MODIS data to the Polar Stereographic projection ~~used by MAR~~ using nearest-neighbour re-sampling, yielding a spatial resolution of $\sim$ 600 x 600 m. When undertaking comparisons with MAR outputs, cloud-free MODIS data were binned into 7.5 km^2 pixels to match MAR's resolution.

We detected bare ice and then dark ice within bare-ice areas by applying thresholds to reflectance values (R) (Shimada et al., 2016). For bare ice we adopted $R_{841-876nm} < 0.6$. To detect dark bare ice we used $R_{620-670nm} < 0.45$. Pilot field

spectra acquired in July 2016 indicate that this slightly higher threshold — compared with $R_{620-670nm} < 0.4$ used by Shimada et al. (2016) — captures dark ice more accurately (Appendix A). However, we note that we do not know precisely what this dark ice threshold represents physically. ~~For instance, we do not know the composition, concentration or sub-pixel spatial distribution of LAIs which result in $R < 0.45$, nor whether the threshold represents the minimum amount of darkening required to be detectable either in the field or remotely. Thus, our threshold may not capture all sources of darkening or precisely identify precisely the timings of dark ice dynamics. It is also noteworthy that $R_{620-670nm}$ straddles a transition zone between wavelengths mostly influenced by LAIs and wavelengths mostly influenced by grain evolution and interstitial water~~The red band (620–670 nm) sits within the visible wavelengths and is therefore affected mostly by LAIs rather than grain evolution or water ponding, which mostly affect the near-infrared wavelengths (700–1100 nm). However, we caveat that other mechanisms can also reduce the reflectance across the entire solar spectrum, including in the red wave-band. These include reduction in volume-scattering due to wind or water 'polishing' the ice surface, infilling of interstitial air spaces with meltwater, and 'trapping' by roughness features such as crevasses. Nevertheless, by combining these thresholds we are able to distinguish at first order between clean and dark (LAI-laden) ice surfaces.

2.2 Selection of common area

We defined a common area of maximum dark ice extent. This enabled the spatial sampling area to be held constant when calculating inter-annual statistics. We chose this approach over defining different areas of dark ice for each year because then the spatial sampling area would have changed dramatically from one year to the next, whereas we are mainly interested in the primary drivers of inter-annual variability in dark ice dynamics.

To define the common area, first, in each year, we identified the pixels which were flagged as dark on at least 10 d during June-July-August (JJA). Then, we retained only those pixels which went dark in at least 4 y of our time series. Finally, we removed all dark pixels which occurred within ∼1 km of the ice sheet margin as defined by the Greenland Ice Mapping Project (GIMP; Howat et al., 2014) in order to remove errant pixels consisting of mixed land and ice cover which remained after applying the GIMP ice area mask. The common area is depicted in Fig. 1 and covers ∼10,400 km^2.

2.3 Metrics of dark ice dynamics

We derived four metrics to characterize spatio-temporal variations in dark ice. First, annual extent (D_E) corresponds to ~~all~~ the extent (in km^2) covered by the pixels within the common area which were dark for at least 5 d in each year. Second, annual duration (D_D) was defined at each pixel in the common area as the percentage of ~~all~~ daily cloud-free observations made in each JJA period which were classified as dark, and is thereby normalised for cloud cover. Third, intensity (D_I) was defined as the mean daily reflectance over 620–670 nm of all cloud-free pixels in the common area, and annual intensity ($\bar{D}_I$) as the ~~mean of all days in each JJA period~~JJA mean of D_I. A lower value of D_I or $\bar{D}_I$ therefore means that dark ice intensity was greater. D_I is on a continuous scale and so is independent of the stringent dark ice presence threshold defined in Sect. 2.1.

Only days in which at least 50 % of the common area was cloud-free were included in the calculation, and only the cloud-free pixels within the common area were used. Fourth, normalised darkness (D_N) was expressed as

$$D_N = \frac{D_D}{\bar{D_I} \cdot 100} \tag{1}$$

and therefore provides a combined indicator of both the duration and intensity of dark ice presence.

We note that cloud cover was present to some degree over the common area in almost every day of our time series, which prevented us from quantifying daily dark ice extent.

2.4 Timing of bare ice and dark ice appearance

At each pixel and for each year we identified the date on which (a) bare ice emerged from underneath the melted snowpack (t_B) and (b) dark ice appeared (t_D), if at all. In both cases we used a 7 d rolling window on the relevant time series of reflectance at each pixel. Each year, we identified the first rolling window at each pixel that contained at least 3 days of bare or dark ice (not necessarily consecutive) ~~, with any remaining days~~ and 0 days of non-bare or non-dark ice, which therefore permitted up to 4 days of cloud cover in the window~~only allowed to be cloudy~~. We then selected the first day of bare or dark ice appearance from within the chosen window. This windowing strategy enabled us to minimise the likelihood of false-positive identification of bare and dark ice appearance dates which would have occurred if only looking at daily observations in isolation and also allowed us to ameliorate for cloud cover.

Finally, we calculated the median and inter-quartile range (25th percentile and 75th percentile) of the day-of-year of bare ice appearance for the common area each year ($\tilde{t_B}$) from the pixel-level data.

2.5 Meteorological and climatological data

We performed simulations of meteorological conditions over the GrIS using version 3.6.2 of Modèle Atmosphérique Régional (MAR), a regional climate model (Fettweis et al., 2017). The model was run on an equal-area 7.5 x 7.5 km resolution grid for the whole of Greenland and was forced at its boundaries every 6 h by ECMWF ERA-Interim re-analysis data (Dee et al., 2011) . For comparison with dark ice dynamics we down-sampled the MODIS-defined common area to MAR's resolution. We calculated mean shortwave-down ($SW\downarrow$), longwave-down ($LW\downarrow$), and sensible heat flux (SHF) anomalies (positive when into the ice sheet surface) in the common area for each JJA relative to 1981–2000. We also calculated the mean daily snow depth in the common area from April to August each year, total snowfall (from $\tilde{t_B}$ to 31 August) and total rainfall (during JJA).

We characterised near-surface air temperatures in two ways. First, we defined the mean air temperature during JJA as T. Second, we defined the number of days in each JJA period ~~on~~ in which the common area's daily *minimum* near-surface air temperature exceeded 0 °C as ~~$\sum T > 0$~~$\sum(T > 0)$.

As introduced previously, cryoconite holes form and tend to be sustained under $SW\downarrow$ dominant conditions. ~~This~~ Conversely, this suggests that they are likely to melt out, depositing cryoconite onto the ice surface, if the surface energy balance shifts to

$LW\downarrow$ or SHF dominant conditions. We therefore ~~estimated the daily energy available to cause the~~ characterised the conditions which could cause melt-out of cryoconite holes as the 'melt-out flux', MOF, using

$$SW_{net} = SW\downarrow \cdot (1-\alpha) \tag{2}$$

$$LW_{net} = LW\downarrow - LW\uparrow \tag{3}$$

$$MOF = SHF + LW_{net} - SW_{net} \tag{4}$$

where α was the daily mean MOD10A1 albedo over the common area (only on days with <50 % cloud cover) and $LW\uparrow$ was 315.6 $\mathrm{Wm^{-2}}$ for melting ice surfaces as defined by Cuffey and Paterson (2010). SHF is positive when into the ice sheet surface. $\bar{MOF}$ corresponds to the mean JJA MOF.

We used the monthly Greenland Blocking Index (GBI) (Hanna et al., 2016) to consider the role of the synoptic atmospheric circulation in dark ice dynamics. The GBI is the mean 500 hPa geopotential height for the 60–80 °N, 20–80 °W region and therefore provides a measure of the extent of high-pressure blocking over Greenland. We calculated the mean GBI for each JJA period.

~~We tested for relationships between metrics of dark ice dynamics and meteorology using ordinary least squares regression.~~

3 Results

3.1 Characteristics of dark ice dynamics

Shimada et al. (2016) identified a general trend of increasing D_E over time but also saw that D_E on the south-west GrIS varied dramatically between years. We found similar characteristics in our expanded time series (Fig. 1). D_E ranged from almost no dark ice identified (2000, 2001 and 2015), to wide, contiguous areas of dark ice stretching from 65.5 to 69°N (2007, 2010, 2011, 2012, 2014 and 2016).

~~In addition, there~~ There was substantial inter-annual variability in D_D during JJA. Generally, when D_E was high, D_D was also high, especially in 2010, 2012 and 2016. Moreover, the extension of our time series relative to Shimada et al. (2016) which only examined July to encompass June through August revealed relatively large D_E and D_D in 2005, 2007, 2008, 2009, 2011 and ~~2014 which has not been captured previously.~~ 2014.

Examination of D_I (Fig. 2) shows that most dark ice presence was concentrated into the months of July and August. In some years (2010 and 2016) more significant darkening of the ice sheet surface was observed as early as mid June. In years when substantial darkening occurred there was a time lag ~~following~~ between $\tilde{t_B}$ and the first widespread occurence of dark ice of ∼10–15 d, although in some cases (e.g. 2010) this may be attributable to the large inter-quartile range in date of bare ice appearance (Fig. 2. D_I tended to increase over the season. Variability in D_I at daily to weekly timescales was minimal compared to the magnitude of variability over inter-annual timescales. Dark ice usually persisted until the onset of anti-cyclonic, cloudy conditions (Fig. 2, days shaded ~~gray~~grey) and snowfall during late August and September, which buried the bare-ice surface under snowpack for the winter period.

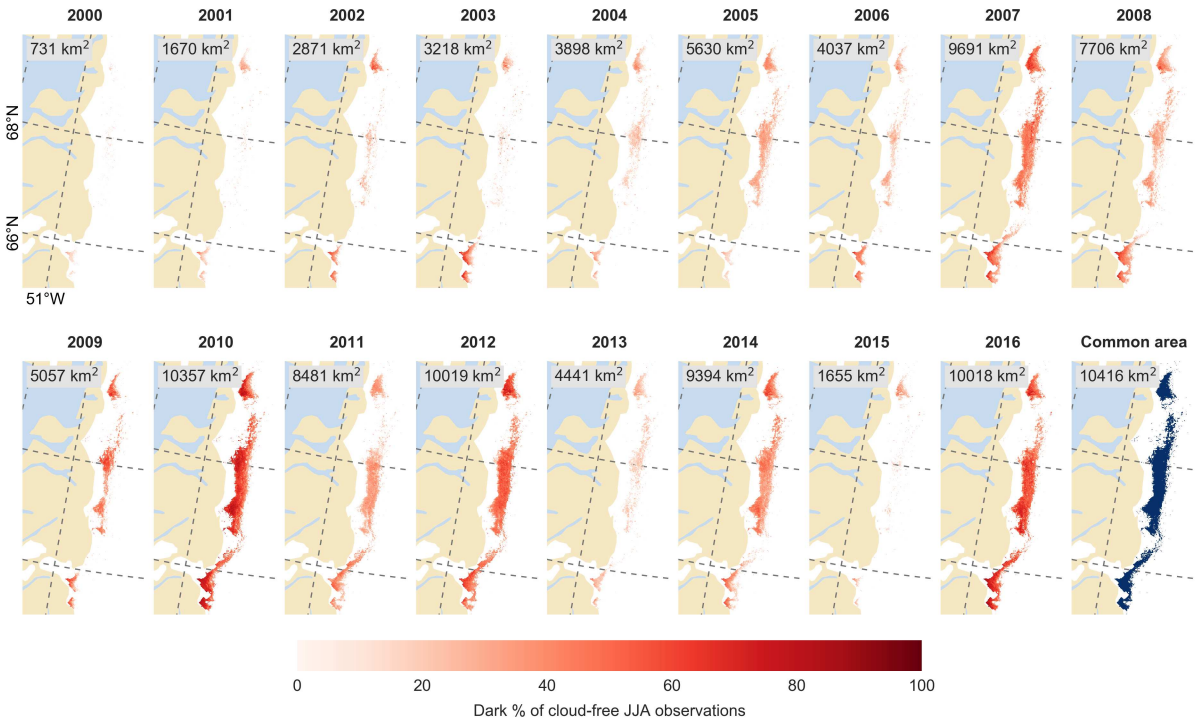

Figure 1. ~~D_E and~~ D_D on the south-west GrIS each summer from 2000 to 2016, expressed as a percentage of the total daily cloud-free observations made during June-July-August (JJA). Each year is labelled with D_E. In each year, pixels that are dark for fewer than 5 days are not shown. Bottom-right panel: common area of dark ice used for inter-annual comparisons.

We did not find any evidence that the dynamics of dark ice in one year controlled dark ice dynamics the following year. There were ~~been~~ years of higher D_N recently (2012, 2014, 2016) interspersed with years of much lower D_N (2013, 2015). Moreover, D_I values at end of one melt season were generally significantly different to those in the period after $\tilde{t_B}$ the following year (Fig. 2).

We used t_D to calculate cumulative D_E in the common area through the summer (Fig. 3, red lines). In several years D_E was very small (2000, 2001, 2003, 2015). In years when medium D_E occurred (e.g. 2005, 2006, 2008, 2009, 2013), dark ice appeared step-wise through July and into August. This step-wise appearance also occurred in the high D_E years of 2007 and 2010. In contrast, the widespread expansion of D_E in 2011, 2012, 2014 and 2016 occurred rapidly over just a few days in July. In particular, we found 28 large, single-day expansions in dark ice extent in our time series (defined as >520 km^2, equivalent to $\sim$5 % of the common area). These large changes ~~were not explicable~~ cannot be explained by gaps in our time series owing to cloud cover: the median number of preceding days when cloud cover was >50 % was 0, and the mean common area covered by cloud in the preceding 7 days was 34 %. There tended to be minimal further dark ice expansion in August. As shown by

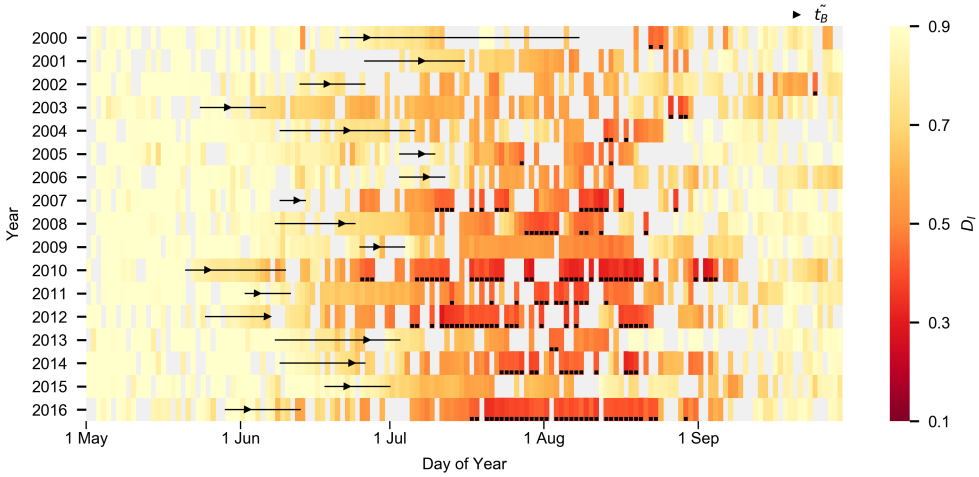

Figure 2. D_I in the common area during May to September from 2000 to 2016. Only days on which at least 50 % of the common area is cloud-free are shown. Black squares denote days on which the ~~entire~~ average dark ice intensity, D_I of the cloud-free common area ~~had D_I <~~ was <0.45. Black triangles denote the date of snow clearing, $\tilde{t_B}$. Horizontal black bars denote the inter-quartile range of the day-of-year of bare ice appearance.

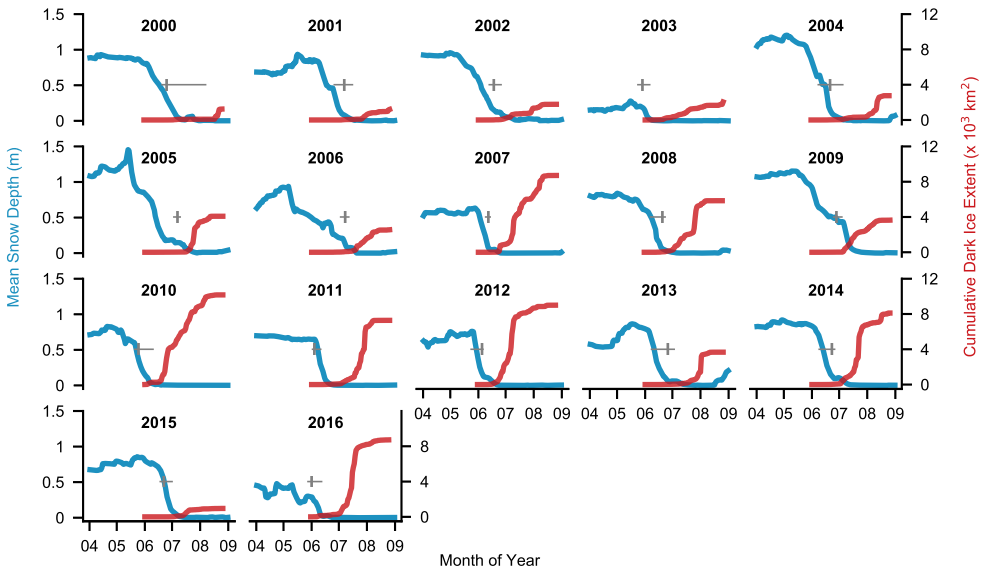

Figure 3. Average snow depth (blue) and cumulative dark ice extent, D_E (red) in common area during April to August each from 2000 to 2016. Vertical bars (grey) denote $\tilde{t_B}$; horizontal bars (grey) denote the inter-quartile range of the day-of-year of bare ice appearance.

D_E (Fig. 1) and D_I (Fig. 2), the ~~magnitude~~ extent and intensity of dark ice tended to persist for the rest of the summer season (Figs. 1 and 2).

3.2 Controls on dark ice presence

In years when ~~the ice went dark then t_D and~~ D_E was higher then D_D (Fig. 1) and t_D (Fig. 3) tended to be spatially invariant across the common area. This suggests that the driver/s of dark ice presence is/are synoptic, governing dark ice dynamics over the whole common area. We therefore used meteorological and climatological variables representative of the common ~~dark ice~~ area to examine their potential impact upon dark ice dynamics.

3.2.1 Snow

Snow can control dark ice dynamics in at least two major ways: (a) the thickness of the snowpack from the preceding winter will, in combination with air temperatures, control $\tilde{t_B}$; and (b) snowfall ~~which~~ that occurs during the melt season will at least temporarily obscure the bare ice surface.

Fig. ~~2 shows $\tilde{t_B}$ and Fig.~~ 3 shows the mean snowpack depth and t_B from April through to August each year. In the years of longest D_D and greatest D_I (2007, 2010, 2012, 2016) bare ice appeared by roughly mid June according to both MODIS and MAR, compared to other years when bare ice did not appear until early to mid July.

Earlier $\tilde{t_B}$ is not just a function of total snowfall during the preceding winter but is also strongly dependent on the progression of melting during spring which, in extreme cases such as 2016, began as early as April, introducing liquid water to the snowpack and accelerating its warming despite additional snowfall in May. On the other hand, in years such as 2015, significant melting did not occur for the first time until mid June. Not only was 2014–2015 winter snowfall relatively large compared to other years in our study, but more snowfall occurred around the start of June just before the melt season started. Nevertheless, in general a thinner winter snowpack favoured earlier $\tilde{t_B}$, and earlier $\tilde{t_B}$ in turn favoured increased D_N (R^2 0.51, $p < 0.01$, Fig. 5f). Last, when further snowfall occurred during summer (Fig. 4b) then D_N tended to be lower (R^2 0.36, $p < 0.05$).

3.2.2 Atmospheric energy fluxes

$SW\downarrow\prime$ was consistently positive from 2007 onwards but continued to show substantial inter-annual variability (Fig. 4a). There was no statistically significant relationship between JJA $SW\downarrow\prime$ and D_N. Unlike $SW\downarrow\prime$, from 2000 to 2007 $LW\downarrow$ anomalies were consistently positive and then after 2007 the sign became more variable, with both positive and negative anomalies occurring (Fig. 4a). Like $SW\downarrow\prime$ there was no statistically significant relationship with D_N.

$SHF\prime$ was consistently positive throughout the time series. There was a significant positive correlation between $SHF\prime$ and D_N (R^2 0.41, $p < 0.01$, Fig. 5e).

We examined the likelihood for cryoconite hole melt-out (causing redistribution of cryoconite materials onto the ice sheet surface) using $M\bar{O}F$ (Fig. 4c), which ~~describes the amount of energy available~~ is suggestive of the energy balance conditions that are needed to melt cryoconite holes out of their weathering crust. Positive $M\bar{O}F$ signifies that longwave and sensible heat fluxes dominate the energy balance, which ~~will~~ could cause spatially 'even' surface melting as opposed to spatially heterogeneous melting permitted by stronger absorption of $SW\downarrow$ where cryoconite material is present. $M\bar{O}F$ was negative in

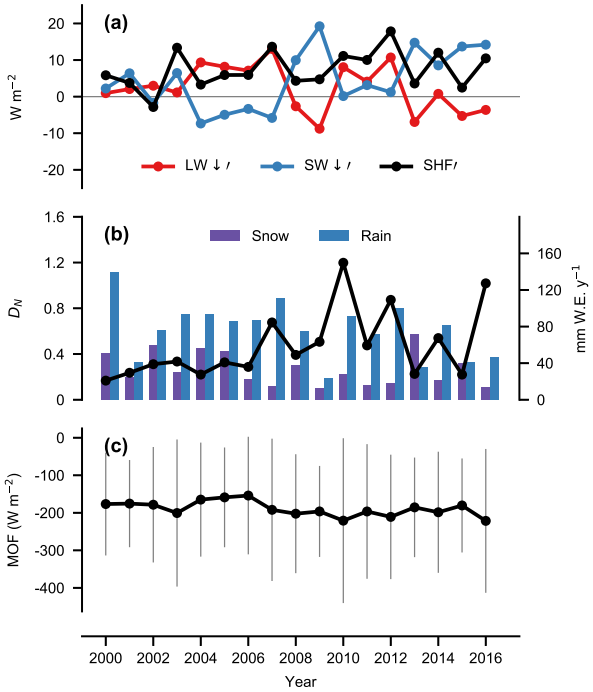

Figure 4. JJA meteorology and D_N from 2000 to 2016. (a) $SW\downarrow\prime$, $LW\downarrow\prime$ and $SHF\prime$ (see Sect. 2.5). (b) Normalised darkness (D_N), total snow inputs from ~~date of snow clearing~~ $\tilde{t_B}$ until 31 August and rain inputs during JJA. (c) $\bar{MOF}$, $\pm 3\sigma$ (see Sect. 2.5).

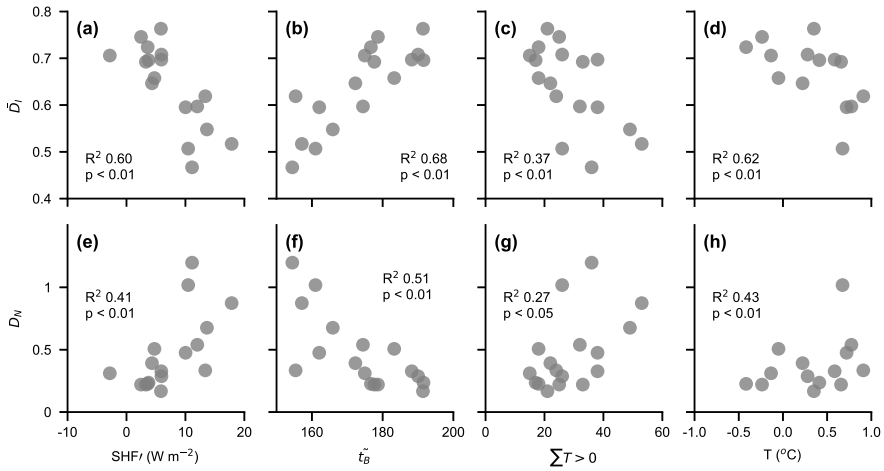

Figure 5. Relationships between meteorological indicators and dark ice intensity, D_I (upper) and normalised darkness, $\bar{D_N}$ (lower).

all years, and all days within 3σ of the mean were also negative, which suggests that the positive $M\bar{O}F$ conditions required for the widespread melt-out of cryoconite holes were seldom (if ever) met.

As liquid meltwater constitutes a pre-requisite for algal growth, we assessed the likelihood of continuous liquid meltwater presence on the ice surface over each 24 h cycle using $\sum T > 0$ $\sum(T > 0)$. We found a positive correlation between $\sum T > 0$ $\sum(T > 0)$ and $\bar{D}_I$ (R^2 0.37, $p < 0.05$, Fig. 5c) and to a lesser extent with D_N (R^2 0.27, $p < 0.05$, Fig. 5g). Greater $\sum T > 0$ coincided with higher SHF $\sum(T > 0)$ were associated with higher SHF (R^2 0.55, $p < 0.01$). Moreover, we found that single days of large dark ice area expansion were associated with a median of 3 days of continuous (24 h) melting, compared to 0 days for the rest of the time series. These sudden increases in dark ice extent were associated with higher absolute sensible heat fluxes, with a mean of 57±24 $\mathrm{Wm^{-2}}$, equivalent to 96% more sensible heat than on the days the SHF mean in the period from the start of dark ice expansion until a maximum D_E of 90 % of the common area. Over daily timescales, higher SHF was associated with warmer near-surface air temperatures (R^2 0.54, $p < 0.01$) but more strongly with higher near-surface wind speeds (R^2 0.67, $p < 0.01$). Days on which the minimum air temperature was greater than 0 °C had mean wind speeds of 6.5 ± 1.8 $\mathrm{ms^{-1}} \pm 1\sigma$, compared to 4.9 ± 1.3 $\mathrm{ms^{-1}} \pm 1\sigma$ on days when the minimum air temperature was 0 °C or less.

Last, we examined whether the dark ice dynamics have any relationship with the GBI. We found a positive correlation between the JJA GBI and D_N (R^2 0.46, $p < 0.05$).

3.2.3 Rainfall

Rainfall can occur in the ablation zone of the GrIS during summer. Limited observations from elsewhere in the cryosphere indicate that whilst the direct melt impact of rainfall upon melt rates is generally limited, rain can affect melt indirectly by increasing the liquid water content of the ice surface, reducing its albedo (Hock, 2005). Total JJA rainfall in this sector ranged from 30 mm w.e. to as much as 140 mm w.e. (Fig. 4b). However, there was no statistically significant relationship between JJA total rainfall and D_N.

Eyewitnesses on the ice sheet surface have observed that the weathering crust generally widespread porous surface weathering crust, typically in the order of 20–30 cm deep, can be stripped back to down towards the underlying high-density bare ice during rainfall events (potentially dispersing cryoconite material) but from cryoconite holes). However, they also observed that it tends to reform within daysthicken again within days, due primarily to renewed subsurface melt by incoming shortwave radiation (Cook et al., 2016b). We therefore also examined the impact of each JJA rainfall event upon D_I. We selected all rainfall (and snowfall) events of >1 mm W.E. $\mathrm{d^{-1}}$ across our common area in our time series. Then, we calculated the change in D_I using the closest observations immediately before and after the rainfall event. We found no systematic change in D_I caused by rainfall events: in some cases D_I increased while in other cases it decreased. This was the case whether or not mixed rainfall and snowfall events were excluded from analysis, although we note that MAR may not adequately discriminate between rainfall and snowfall over ice surfaces.

4 Discussion

At outlined in Sect. 1, a number of processes have been proposed to explain the dark ice dynamics on the south-west of the GrIS. Our characterisation of dark ice in terms of D_E, D_D, D_I and t_D, when combined with analysis of the prevailing meteorological conditions estimated by MAR, allows us to consider the extent to which each proposed process fits with our observations of dark ice dynamics.

4.1 Variability driven by inorganic particulate deposition or redistribution

There are two primary ways in which inorganic particulate matter can arrive on the ice-sheet surface: (1) by wet and dry atmospheric deposition, and (2) ~~melt-out of material~~ deposition of material previously trapped in the ablating ice. Previous research indicates that there is no relationship between albedo reductions and the number of fires occurring over North America and Eurasia nor with modelled atmospheric aerosol fluxes (Tedesco et al., 2016). ~~The only published measurements~~ Measurements of black carbon ~~on the GrIS are from~~ in snow on the present-day surface of the GrIS (as opposed to in ice cores) have been made in the north-west (Aoki et al., 2014; Polashenski et al., 2015) and high in the accumulation zone (Hegg et al., 2010; Doherty et al., 2013) . However, at only a few ppb~~are too low~~ , these measurements of black carbon are insufficient to explain the ~~observed~~ substantial reduction in reflectance in the south-west (c.f. Warren, 2013) .

Atmospheric deposition events would presumably have to occur in only years of high D_N in order to explain the spatio-temporal patterns in dark ice that we observed. In dark years, D_I increased gradually over the summer and so we postulate that deposition would need to occur over at least several days after $\tilde{t_B}$. More problematic is that maximum D_E is relatively invariant and begins c. 20 km inland rather than at the margin, whereas atmospheric deposition would presumably occur over a more dispersed area.

The well-defined geometry of the dark-ice area between years lends support to the hypothesis that the dark-ice area is caused by ~~the melt-out of particulates~~ surface deposition of particulates previously trapped in the ablating ice (Wientjes and Oerlemans, 2010; Wientjes et al., 2012). Warmer air temperatures in darker years (R^2 0.43, $p < 0.01$; Fig. 5d/h) support the idea that more material ~~can melt out~~ is deposited on the surface from melted ancient ice in these years~~and thereby contribute to darkening ,~~ , contributing to darkening and possibly acting as a positive feedback mechanism. However, our dynamics observations suggest that ~~particulate melt-out is~~ particulates from ancient ice are not the primary source of darkening. First, there is more variability in D_E and D_D than we would expect if total summer ablation alone determined darkening by controlling the corresponding quantity of particulates ~~melting out~~being released from ancient ice. D_E was negligible in several years (Fig. 1), yet melting in this area occurred in all years (e.g. van den Broeke et al., 2011; van As et al., 2016). Second, particulates are unlikely to be dispersed homogeneously through the ice column and so the concentration of ~~melt-out~~ particulates emerging at the surface will change non-linearly with respect to the ice-melt rate. This could explain why D_E is negligible in several high-melt years. However, the wavy patterns of surface darkening at ~~decimetre~~ decametre scales observed by Wientjes and Oerlemans (2010) are indicative of dispersion of previously well-defined particulate horizons by vertical shear due to ice flow, which suggests that particulates ~~melted out~~ from ancient ice were deposited in each summer of our time series. Third and most critically, in

order to explain non-dark years such as 2013 and 2015, the particulate material responsible for substantial darkening during 2010–2012 and 2014 would have to be evacuated from the ice-sheet surface at the end of summer to explain both dark ice that summer and the lack of dark ice the year after. More broadly, we did not find a year-on-year increase in D_I that we would expect if ~~melt-out particulates~~ particulates from ancient ice were accumulating at the ice-sheet surface (Fig. 2). We also found that in years of high D_N the onset of high D_I was delayed by ∼10-15 d after $\tilde{t_B}$ (Fig. 2). This may be attributable to remaining snow patches or superimposed ice formation~~but~~ , although the prevalence of ~~this~~ the latter process on the GrIS remains poorly understood ~~(Larose et al., 2013; ?)~~ (Larose et al., 2013; Chandler et al., 2015) . Nevertheless, if particulate materials were still present on the surface from the previous melt season we would expect high D_I almost immediately after bare ice appearance.

Overall, our observations provide little support to the hypothesis that particulate deposition causes surface darkening. We are unable to identify a mechanism by which the ice-surface mass flux of particulate material could change over timescales commensurate with dark ice dynamics.

4.2 Variability driven by cryoconite hole processes

Shimada et al. (2016) hypothesised that the opposing processes of cryoconite hole formation (under $SW\downarrow$ dominant conditions) versus melt-out (under $LW\downarrow$ dominant conditions) could explain inter-annual variability in D_E.

There are several noteworthy limitations to investigating cryoconite hole processes from satellite observations. First, cryoconite hole processes occur over decimetre scales and so we may not be able to capture their variability using 500 m MODIS imagery. Second, the reflectance of ice surfaces with cryoconite holes varies strongly as a function of viewing angle (Bøggild et al., 2010), and so observations made by MODIS — which has a 'push-broom' scanning assembly — will vary depending on how near to nadir the angular Instantaneous Field Of View (IFOV) is. This is likely to impact the broadband albedo value from MOD10A1 used to calculate SW_{net} as part of MOF in a way that is not currently known.

Shimada et al. (2016) suggested that low D_E in July 2011 followed by widespread D_E in July 2012 could be attributable to cryoconite hole wash-out during anti-cyclonic conditions in late August and September 2011. However, our results reveal a different spatio-temporal pattern of darkening: we found that the common area did go dark in 2011, but that this did not begin until late in July. Maximum D_I was reached during August, which Shimada et al. (2016) omitted from their analysis. In 2012 we observed an early onset of high D_E, with rising D_I as the season continued, whereas under a return to $SW\downarrow$ dominant conditions we would expect D_I to gradually decrease as cryoconite hole surfaces deepen, albeit non-linearly because cryoconite holes cease deepening once they are in equilibrium with their surroundings (Gribbon, 1979). This also makes it difficult to explain low D_E in 2013, as cryoconite holes would have needed to form over a short period at the end of summer 2012 in order to sequester cryoconite particles at depth, unless the presence of snow patches and/or superimposed ice at the surface was so prolonged that only in a few pixels did enough melting take place to expose bare/dark ice.

We also looked at intra-annual variations in dark ice dynamics when considering the potential for variability to be driven by cryoconite hole processes. Field observations of cryoconite hole morphology show that cryoconite holes form within the ice weathering crust over timescales of a few days (Cook et al., 2016a). However, in dark years, t_D was relatively synchronous across the common area. Importantly, D_I then increased as the season continued, suggesting that episodic cryoconite hole

flushing and reformation is unlikely. This is supported by field observations made in the south-west ablation zone of the GrIS by Chandler et al. (2015) , who found that cryoconite hole coverage increased over the course of the 2015 melt season despite transiently warm, cloudy conditions experienced during July that caused some holes to melt out and release their debris. Moreover, the lack of energy available for cryoconite hole melt-out over seasonal timescales (Fig. 4c) suggests that variability in the areal extent of cryoconite holes forced by changes in the dominant component(s) of the surface energy balance cannot explain dark ice dynamics. Our only evidence in support of cryoconite hole processes is that large single-day increases in dark ice extent were associated with higher absolute SHF, which could ~~still~~ cause transient hole-flushing events during the melt season. However, the rest of our evidence strongly suggests that cryoconite hole processes are not responsible for inter-annual dark ice dynamics.

4.3 Variability driven by ice algal assemblages

Last, we examined evidence for the role of ice algal assemblages as the principal driver of dark ice dynamics. In addition to typical light-harvesting pigments characteristic of green microalgae (Remias et al., 2009), ice algae produce a unique UV-VIS absorbing purpurogalin pigment that presumably affords protection from the significant radiation experienced in GrIS surface habitats (Remias et al., 2012). Given this pigmentation, ice algal blooms are known to impact visible reflectance at local (metre) scales (Yallop et al., 2012; Lutz et al., 2014). Knowledge of the regulation of temporal and spatial patterns in ice algal biomass (and thus pigmentation) in surface habitats is limited (Yallop et al., 2012; Chandler et al., 2015), but the fundamental pre-requisites for algal life are known, including liquid water, nutrient resources and photosynthetically active radiation (PAR, 400–700 nm).

The significant positive relationship identified between ~~$\sum T > 0$~~ $\sum(T \geq 0)$ and D_I (R^2 0.37, $p < 0.01$, Fig. 5g) supports the role of ice algae in ice sheet darkening, as do the single-day increases in D_E of >5 % of the common area, which were generally preceded by several days of continuous positive air temperatures; both of these observations are indicative of liquid meltwater presence. Ice algae require liquid water in order to grow, and ice surfaces are reservoirs of potentially viable propagules that can become active when they encounter sufficient liquid water of appropriate chemistry (Webster-Brown et al., 2015). Minimum air temperatures above 0°C required for the presence of liquid water will facilitate growth of ice algae. As blooming progresses, the relationship between liquid water availability and algal proliferation may be strengthened by the establishment of a positive feedback loop via albedo reduction. For example, blooms of snow algae have been shown to result in surface albedo reduction, increased heat retention at the snow surface, and thus enhanced melting and liquid water availability for continued algal growth (Lutz et al., 2016). Climatically, enhanced liquid meltwater presence in dark years — especially continuing through the night when $SW\downarrow$ tends to zero — is also partially attributable to increased $SHF\prime$, with a positive correlation observed between $SHF\prime$ and D_N (R^2 0.41, $p < 0.01$, Fig. 5e) in our study. Thus a combination of greater ~~$\sum T > 0$~~ $\sum(T \geq 0)$ and higher $SHF\prime$ may regulate inter-annual liquid water availability in ways critical to ice algae growth, thereby governing whether or not dark ice appears.

$\tilde{t_B}$ has a first-order impact on whether the common area is dark in any given year, with later appearance associated with lower D_E (Fig. 5b,f). $\tilde{t_B}$ will significantly impact PAR availability at the ice surface. If bare ice appears in early to mid June,

it will receive PAR over several complete diurnal cycles, unlike in years when bare ice does not appear until July. Although ice algae likely experience excessive irradiance over the ablation season, as evidenced by their production of 'sun-screen' pigments (Remias et al., 2012), a minimum threshold of PAR (or photo-period duration) may be required to allow bloom initiation, which would be favoured by earlier $\tilde{t_B}$. Alternatively, variability in $\tilde{t_B}$ may impact algal blooms (and thus darkening) via the timing of nutrient inputs to surface ice, or due to the formation of superimposed ice. With delayed snow line retreat, percolating snow melt in spring/early summer may release snow pack nutrients to surface ice (Larose et al., 2013) before PAR is available to allow algal utilisation, stalling bloom formation. It may also result in sustained presence of superimposed ice (Larose et al., 2013; Chandler et al., 2015), preventing PAR penetration to the previous year's ice algal cells and initiation of growth. However, we found no significant relationship between $SW\downarrow\prime$ (which corresponds approximately to PAR) and D_N, so the role of seasonal PAR fluxes in algal growth remains unclear. More broadly, field studies are required in order to identify precisely ~~how bare ice appearance~~ the transition from snow to a bare-ice surface could impact ice algal assemblages.

If pre-requisites for the initiation of an algal bloom are achieved then an increase in algal biomass is likely, with a concomitant increase in D_I. This is consistent with increases in D_I after the first appearance of dark ice, as opposed to 'flickering' between less- and more- dark states. Increases in D_I could be driven by an increase in the spatial extent of ice algal assemblages and/or an increase in algal concentrations per unit area, although we note that increases in D_I which occur immediately after snow retreat could also be due to the melting away of superimposed ice (e.g. Larose et al., 2013) . Previously, Chandler et al. (2015) recorded an increase in 'dirty ice' extent within our common area over an ablation period, though they did not assess algal cell numbers within dirty ice. Whilst algal concentrations likely increase until a limiting factor becomes apparent, analogous to algal blooms in aquatic systems (Teeling et al., 2016), progressive colonisation of clean ice at the sub-MODIS pixel scale would still result in continued increases in D_I at the regional scale. Indeed, we do not know how much of a given MODIS pixel must be covered in a light algal bloom before the pixel reflectance dips below the dark ice threshold~~. Given~~ , nor how much of an impact processes such as overnight refreezing of the ice surface will have on diurnal variability in reflectance. Such considerations are particularly important when considering variations in area-wide D_I above and/or within a few percent of the field-derived reflectance threshold of 0.45, as physical changes in the weathering crust (e.g. liquid water content) will also force variations in D_I independently of variability in algal growth. Lastly, given the confounding impacts of cloud cover on MODIS observations, assessing the relative contribution of increases in the extent (D_E) versus concentration of algae (D_I) on regional variability in dark ice dynamics is not possible. We suggest, however, that intra-annual patterns in D_I over ablation periods are more consistent with the progression of ice algal blooms than with dynamics in other darkening agents previously discussed.

We interpret our observations as support for the role of ice algae in controlling inter-annual dynamics in darkening, but note that there is currently not sufficient evidence to formally test this assertion. In particular, one major aspect of dark ice variability which ice algae cannot explain is the well-defined maximal spatial extent of dark ice, both in the south-west and GrIS-wide. ~~Dark ice extent is concentrated spatially into several contiguous areas around the GrIS (Shimada et al., 2016) .~~ However, if algal growth were the only factor causing inter-annual variability in dark ice presence, we would expect to see dark ice present wherever the climatological pre-requisites for algal growth are met. These climatological pre-requisites can be

found elsewhere, most notably in the 20 km-wide zone from the ice-sheet margin to the start of the common area examined in this study. This suggests that algal growth controlled by climatology alone cannot fully explain dark ice dynamics in the south-west sector of the GrIS. In light of our findings, we hypothesise that inter-annual variability in dark ice presence — both in the south-west sector and GrIS-wide — requires (1) ~~melt-out of particulates~~ particulates outcropping from ancient ablating ice and (2) blooming of ice algal assemblages. Specifically, we suggest that the ~~in-situ melt-out of~~ outcropping particulates defines the spatial extent of dark ice. Algal blooms ~~control~~ are likely to exert a control on dark ice intensity ~~by enhancing the abiotic darkening signal~~in areas where outcropping particulates are present, but only when the climatological pre-requisites for growth are also met. For our hypothesis to be correct, ~~melt-out~~ outcropping particulates must enable ice algae growth of sufficient magnitude to cause appreciable darkening, for instance as a source of nutrients, but they do not need to be present in high enough concentrations to cause darkening by themselves, nor do they need to have mineralogical characteristics that appear dark in the visible spectrum. In addition our observations imply that over inter-annual timescales in the south-west GrIS, outcropping dust is always present, due either to continuous delivery or to long residence times. This is unlikely to hold over longer timescales if darkening by algal assemblages is contingent on the delivery of outcropping dust from ancient ablating ice.

5 Conclusions

We detected hitherto overlooked dynamics of the dark ice zone of south-west of the GrIS using remotely-sensed imagery. Our results show that GrIS dark ice dynamics must be examined across ~~across~~ the full duration of the melt season in order to understand the processes most likely to be reducing the albedo of bare ice surfaces. We found that in years when the south-west sector of the GrIS darkens, this usually occurs within several days and then remains widespread for the rest of the melt season, indicating that the darkening occurs in response to a common synoptic forcing. The seasons of longest dark ice duration (D_D) tend to be associated with earlier retreat of the winter snowpack. Once the ice goes dark then the dark ice intensity (D_I) tends to increase gradually through the melt season. Daily variations in D_I are fairly small.

In our analysis, the JJA sensible heat flux anomaly and the date of bare ice appearance represent the most important climatic controls on dark ice extent (D_E), D_D and D_I, with higher sensible heat fluxes (associated with higher wind speeds) and earlier bare ice appearance favouring more dark ice. Higher JJA air temperatures and a greater number of days during JJA on which continuous surface melting occurs are also associated with darker years. There is a positive correlation between D_N and the JJA Greenland Blocking Index (R^2 0.46, $p < 0.05$), which indicates that the climatic conditions which drive darker years can be attributed at least partly ~~attributed~~ to the summer presence of high-pressure blocking systems over the ice sheet.

Our observations suggest that neither deposition of particulates nor cryoconite hole processes can independently explain inter-annual variability in dark ice presence. Our observations tentatively support the proposal that algal blooming is the primary cause of albedo reductions in dark years, likely driven by earlier winter snowpack retreat and positive sensible heat flux anomalies. However, climatological controls on ~~biological~~ algal growth alone cannot explain the spatial distribution of inter-annual dark ice presence. We therefore suggest that inter-annual variability in dark ice in the south-west sector of the

GrIS is enabled first by the ~~melt-out of particulates~~ deposition of particulates from melting ancient ice. These particulates play an as-yet unknown role in facilitating the growth of ice algal assemblages, which is also controlled by physical/climatic pre-requisites that remain to be identified conclusively.

Future research has several key challenges. First, the spatial distribution, ~~minerology~~ mineralogy and ice-darkening potential of all ~~melt-out~~ light-absorbing impurities outcropping from ancient ice needs to be quantified. Second, the spatial distribution and hence ice-darkening potential of ice algae needs to be examined not just at plot scales but also at scales of hundreds of metres and more. Third, if algal cells are found to be abundant and to be the primary driver of dark ice, then the physical/climatic and nutrient controls on the growth of ice algae need to be established. Last, all these findings should be assimilated into a ~~physical~~ model of ice surface albedo that can be embedded within a regional climate model, in order to project the impact of dark ice upon runoff from the GrIS during the 21st century.

6 Code availability

The Modèle Atmosphérique Régional (MAR) is an open-source regional climate model. Source code of MARv3.6.2 is available at ftp://ftp.climato.be/fettweis/MARv3.6/.src/.

7 Data availability

Monthly outputs from MAR are available at ftp://ftp.climato.be/fettweis/MARv3.6.2/ for different model domains and resolutions. If daily outputs are required, please email xavier.fettweis@ulg.ac.be. MODIS data are available from the USGS LPDAAC Data Pool (https://lpdaac.usgs.gov/data_access/data_pool).

Appendix A: Choice of spectral thresholds

We validated the spectral thresholds used in this study through comparison to hemispherical-conical reflectance factor (HCRF) measurements made in the field on 19 July 2016 in the vicinity of S6 (67°4′28.6″ N, 49°21′32.4″ W). We made HCRF measurements for three qualitatively identified surface types: (1) white ice, (2) light algal bloom (characterised by a light brown colouration to the ice surface) and (3) heavy algal bloom (characterised by a dark brown colouration to the ice surface). ~~The~~ Subsequent microscopic examination of surface samples confirmed the presence of algal cells, along with a very low concentration of mostly clear quartz particles. The HCRF measurements were made following the HCRF measurement protocol described by Cook et al. (in review, 2017). Briefly, an ASD Field Spec Pro spectral radiometer with an 8 degree fore-optic was positioned 30 cm above the sample surface with a nadir viewing angle. This device measures reflected radiance in the wavelength range 350–2500 nm and therefore senses reflected radiance over about 95% of the solar spectrum. The sample surface was qualitatively homogenous in a buffer zone of at least 30 cm around the viewing footprint of the sensor. We calculated the mean of at least twenty sample replicates, all of which were made within one minute without changing the sensor position. All measurements were acquired within a 2 h sampling window around solar noon, thereby minimising error

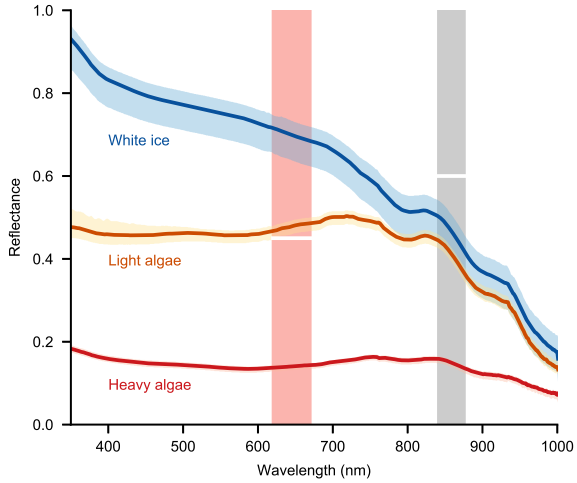

Figure A1. Field HCRF spectra acquired on the GrIS (see Appendix A). For each surface type, solid lines denote mean reflectance and the shaded bounds are delimited by the minimum and maximum reflectances. The ~~gray~~ grey shaded box corresponds to MODIS Band 2 (841–876 nm), and the red shaded box to MODIS Band 2 (620–670 nm). White divisions in each box correspond to the spectral thresholds utilised in this study to define bare and dark ice areas.

due to changing solar zenith. The sky was cloud-free throughout the measurement window. Naturally-illuminated nadir-view HCRF is reported for consistency with the reported MOD09GA data.

The field spectra (Fig. A1) show that the bare-ice threshold used by Shimada et al. (2016) adequately captures white-ice surfaces. Their threshold of $R_{620-670nm} < 0.4$ to define dark ice is conservative and prevents positive identification of light algal blooms. In this study we used a threshold of $R_{620-670nm} < 0.45$, which is set to just below our field observations of light algal bloom reflectance in order to reduce the likelihood of false positives.

Author contributions. A.T., J.B. and M.T. designed the study. A.T. processed the MODIS data, carried out most of the analysis and interpretation and wrote most of the manuscript. J.C. and C.W. contributed to the interpretation and wrote parts of the manuscript. X.F. developed MAR and provided the model outputs. A.H. undertook additional energy balance analysis and contributed to the interpretation. All authors discussed the findings and commented on the manuscript.

Competing interests. The authors declare no competing financial interests. J. Bamber is Advisory Editor of The Cryosphere.

Acknowledgements. This study was supported by the UK Natural Environment Research Council Consortium Grant 'Black and Bloom' (NE/M021025). In addition to the authors, the Black and Bloom team comprises A. Anesio, L. Benning, E. Hanna, S. Hofer, A. Holland, T. Irvine-Fynn, S. Lutz, J. McCutcheon, J. McQuaid, M. Nicholes, E. Sypianska, C. Williamson and M. Yallop.

References

Aoki, T., Matoba, S., Yamaguchi, S., Tanikawa, T., Niwano, M., Kuchiki, K., Adachi, K., Uetake, J., Motoyama, H., and Hori, M.: Light-absorbing snow impurity concentrations measured on Northwest Greenland ice sheet in 2011 and 2012, Bulletin of Glaciological Research, 32, 21–31, doi:10.5331/bgr.32.21, 2014.

Box, J. E., Fettweis, X., Stroeve, J. C., Tedesco, M., Hall, D. K., and Steffen, K.: Greenland ice sheet albedo feedback: thermodynamics and atmospheric drivers, The Cryosphere, 6, 821–839, doi:10.5194/tc-6-821-2012, http://www.the-cryosphere.net/6/821/2012/, 2012.

Bøggild, C. E., Brandt, R. E., Brown, K. J., and Warren, S. G.: The ablation zone in northeast Greenland: ice types, albedos and impurities, Journal of Glaciology, 56, 101–113, doi:doi:10.3189/002214310791190776, http://www.ingentaconnect.com/content/igsoc/jog/2010/00000056/00000195/art00011, 2010.

Cameron, K., Stibal, M., Zarsky, J., Gozdereliler, E., Schostag, M., and Jacobsen, C.: Supraglacial bacterial community structures vary across the Greenland ice sheet, FEMS Microbiology Ecology, 92, 2016.

Casey, K. A., Polashenski, C. M., Chen, J., and Tedesco, M.: Impact of MODIS sensor calibration updates on Greenland ice sheet surface reflectance and albedo trends, The Cryosphere Discussions, 2017, 1–24, doi:10.5194/tc-2017-38, http://www.the-cryosphere-discuss.net/tc-2017-38/, 2017.

Chandler, D. M., Alcock, J. D., Wadham, J. L., Mackie, S. L., and Telling, J.: Seasonal changes of ice surface characteristics and productivity in the ablation zone of the Greenland Ice Sheet, The Cryosphere, 9, 487–504, doi:10.5194/tc-9-487-2015, http://www.the-cryosphere.net/9/487/2015/, 2015.

Cook, J., Hodson, A., Anesio, A., Hanna, E., Yallop, M., Stibal, M., Telling, J., and Huybrechts, P.: An improved estimate of microbially mediated carbon fluxes from the Greenland ice sheet, Journal of Glaciology, 58, 1098–1108, doi:10.3189/2012.JoG12.J001, 2012.

Cook, J., Edwards, A., Bulling, M., Mur, L., Cook, S., Gokul, J., Cameron, K., Sweet, M., and Irvine-Fynn, T.: Metabolome-mediated biocryomorphic evolution promotes carbon fixation in Greenlandic cryoconite holes: Biocryomorphic evolution of cryoconite holes, Environmental Microbiology, 18, doi:10.1111/1462-2920.13349, 2016a.

Cook, J., Hodson, A., Taggart, A., and Mernild, S.: A predictive model for the spectral 'bioalbedo' of snow, Journal of Geophysical Research: Earth Surface, 2016b.

Cook, J., Hodson, A., Gardner, A., Flanner, M., Tedstone, A., Williamson, C., Irvine-Fynn, T., Nilsson, J., Bryant, R., and Tranter, M.: Quantifying bioalbedo: A new physically-based model and critique of empirical methods for characterizing biological influence on ice and snow albedo, The Cryosphere Discussions, doi:10.5194/tc-2017-73, in review, 2017.

Cuffey, K. and Paterson, W. S. B.: The Physics of Glaciers, Butterworth-Heinemann, 3rd edn., 2010.

Dee, D. P., Uppala, S. M., Simmons, A. J., Berrisford, P., Poli, P., Kobayashi, S., Andrae, U., Balmaseda, M. A., Balsamo, G., Bauer, P., Bechtold, P., Beljaars, A. C. M., van de Berg, L., Bidlot, J., Bormann, N., Delsol, C., Dragani, R., Fuentes, M., Geer, A. J., Haimberger, L., Healy, S. B., Hersbach, H., Hólm, E. V., Isaksen, L., Kållberg, P., Köhler, M., Matricardi, M., McNally, A. P., Monge-Sanz, B. M., Morcrette, J.-J., Park, B.-K., Peubey, C., de Rosnay, P., Tavolato, C., Thépaut, J.-N., and Vitart, F.: The ERA-Interim reanalysis: configuration and performance of the data assimilation system, Quarterly Journal of the Royal Meteorological Society, 137, 553–597, doi:10.1002/qj.828, http://dx.doi.org/10.1002/qj.828, 2011.

Dieser, M., Greenwood, M., and Foreman, C.: Carotenoid Pigmentation in Antarctic Heterotrophic Bacteria as a Strategy to Withstand Environmental Stresses, Arctic, Antarctic and Alpine Research, 42, 396–405, doi:10.1657/1938-4246-42.4.396, 2010.

Doherty, S. J., Grenfell, T. C., Forsström, S., Hegg, D. L., Brandt, R. E., and Warren, S. G.: Observed vertical redistribution of black carbon and other insoluble light-absorbing particles in melting snow, Journal of Geophysical Research: Atmospheres, 118, 5553–5569, doi:10.1002/jgrd.50235, http://dx.doi.org/10.1002/jgrd.50235, 2013.

Enderlin, E. M., Howat, I. M., Jeong, S., Noh, M.-J., van Angelen, J. H., and van den Broeke, M. R.: An improved mass budget for the Greenland ice sheet, Geophysical Research Letters, 41, 866–872, doi:10.1002/2013GL059010, http://dx.doi.org/10.1002/2013GL059010, 2014.

Fettweis, X., Box, J. E., Agosta, C., Amory, C., Kittel, C., Lang, C., van As, D., Machguth, H., and Gallée, H.: Reconstructions of the 1900–2015 Greenland ice sheet surface mass balance using the regional climate MAR model, The Cryosphere, 11, 1015–1033, doi:10.5194/tc-11-1015-2017, http://www.the-cryosphere.net/11/1015/2017/, 2017.

Gardner, A. S. and Sharp, M. J.: A review of snow and ice albedo and the development of a new physically based broadband albedo parameterization, Journal of Geophysical Research: Earth Surface, 115, doi:10.1029/2009JF001444, http://dx.doi.org/10.1029/2009JF001444, f01009, 2010.

Gribbon, P. W. F.: Cryoconite holes on Sermikavsak, west Greenland, Journal of Glaciology, 22, 177–181, 1979.

Hanna, E., Cropper, T. E., Hall, R. J., and Cappelen, J.: Greenland Blocking Index 1851–2015: a regional climate change signal, International Journal of Climatology, 36, 4847–4861, doi:10.1002/joc.4673, 2016.

He, T., Liang, S., Yu, Y., Wang, D., Gao, F., and Liu, Q.: Greenland surface albedo changes in July 1981–2012 from satellite observations, Environmental Research Letters, 8, 044 043, http://stacks.iop.org/1748-9326/8/i=4/a=044043, 2013.

Hegg, D. A., Warren, S. G., Grenfell, T. C., Doherty, S. J., and Clarke, A. D.: Sources of light-absorbing aerosol in arctic snow and their seasonal variation, Atmospheric Chemistry and Physics, 10, 10 923–10 938, doi:10.5194/acp-10-10923-2010, http://www.atmos-chem-phys.net/10/10923/2010/, 2010.

Hock, R.: Glacier melt: a review of processes and their modelling, Progress in Physical Geography, 29, 362–391, doi:10.1191/0309133305pp453ra, http://ppg.sagepub.com/cgi/doi/10.1191/0309133305pp453ra, 2005.

Hodson, A., Anesio, A. M., Tranter, M., Fountain, A., Osborn, M., Priscu, J., Laybourn-Parry, J., and Sattler, B.: Glacial Ecosystems, Ecological Monographs, 78, 41–67, doi:10.1890/07-0187.1, http://dx.doi.org/10.1890/07-0187.1, 2008.

Howat, I. M., Negrete, A., and Smith, B. E.: The Greenland Ice Mapping Project (GIMP) land classification and surface elevation data sets, The Cryosphere, 8, 1509–1518, doi:10.5194/tc-8-1509-2014, http://www.the-cryosphere.net/8/1509/2014/, 2014.

Irvine-Fynn, T. D., Bridge, J. W., and Hodson, A. J.: In situ quantification of supraglacial cryoconite morphodynamics using time-lapse imaging: an example from Svalbard, Journal of Glaciology, 57, 651–657, doi:doi:10.3189/002214311797409695, http://www.ingentaconnect.com/content/igsoc/jog/2011/00000057/00000204/art00007, 2011.

Larose, C., Dommergue, A., and Vogel, T. M.: The dynamic arctic snow pack: An unexplored environment for microbial diversity and activity, Biology, 2, 317–330, 2013.

Lutz, S., Anesio, A., Jorge Villar, S., and Benning, L.: Variations of algal communities cause darkening of a Greenland glacier, FEMS Microbiology Ecology, 89, 402–414, 2014.

Lutz, S., Anesio, A. M., Raiswell, R., Edwards, A., Newton, R. J., Gill, F., and Benning, L. G.: The biogeography of red snow microbiomes and their role in melting arctic glaciers, Nature Communications, doi:10.1038/ncomms11968, 2016.

Lyapustin, A., Wang, Y., Xiong, X., Meister, G., Platnick, S., Levy, R., Franz, B., Korkin, S., Hilker, T., Tucker, J., Hall, F., Sellers, P., Wu, A., and Angal, A.: Scientific impact of MODIS C5 calibration degradation and C6+ improvements, Atmospheric Measurement Techniques, 7, 4353–4365, doi:10.5194/amt-7-4353-2014, http://www.atmos-meas-tech.net/7/4353/2014/, 2014.

MacDonell, S. and Fitzsimons, S.: The formation and hydrological significance of cryoconite holes, Progress in Physical Geography, 32, 595–610, doi:10.1177/0309133308101382, http://dx.doi.org/10.1177/0309133308101382, 2008.

Painter, T. H., Duval, B., Thomas, W. H., Mendez, M., Heintzelman, S., and Dozier, J.: Detection of quantification of snow algae with an Airborne Imaging Spectrometer, Applied and Environmental Microbiology, 67, 5267–5272, 2001.

Polashenski, C. M., Dibb, J. E., Flanner, M. G., Chen, J. Y., Courville, Z. R., Lai, A. M., Schauer, J. J., Shafer, M. M., and Bergin, M.: Neither dust nor black carbon causing apparent albedo decline in Greenland's dry snow zone: Implications for MODIS C5 surface reflectance, Geophysical Research Letters, 42, 9319–9327, doi:10.1002/2015GL065912, http://dx.doi.org/10.1002/2015GL065912, 2015GL065912, 2015.

Remias, D., Holzinger, A., and Lutz, C.: Physiology, ultrastructure and habitat of the ice alga Mesotaenium berggrenii (Zygnemaphy- ceae, Chlorophyta) from glaciers in the European Alps, Phyc-ologia, 48, 302–312, 2009.

Remias, D., Schwaiger, S., Aigner, S., Leya, T., Stuppner, H., and Lütz, C.: Characterization of an UV- and VIS-absorbing, purpurogallin-derived secondary pigment new to algae and highly abundant in Mesotaenium berggrenii (Zygnematophyceae, Chlorophyta), an extremophyte living on glaciers, FEMS Microbiology Ecology, 79, 638–648, doi:10.1111/j.1574-6941.2011.01245.x, http://dx.doi.org/10.1111/j.1574-6941.2011.01245.x, 2012.

Rignot, E. and Kanagaratnam, P.: Changes in the velocity structure of the Greenland Ice Sheet, Science, 311, 986–90, doi:10.1126/science.1121381, http://www.ncbi.nlm.nih.gov/pubmed/16484490, 2006.

Rignot, E., Velicogna, I., van den Broeke, M. R., Monaghan, A., and Lenaerts, J.: Acceleration of the contribution of the Greenland and Antarctic ice sheets to sea level rise, Geophys. Res. Lett., 38, 1–5, doi:10.1029/2011GL046583, http://www.agu.org/pubs/crossref/2011/2011GL046583.shtml, 2011.

Sasgen, I., van den Broeke, M., Bamber, J. L., Rignot, E., Sorensen, L. S., Wouters, B., Martinec, Z., Velicogna, I., and Simonsen, S. B.: Timing and origin of recent regional ice-mass loss in Greenland, Earth Planet. Sci. Lett., 333, 293 – 303, doi:10.1016/j.epsl.2012.03.033, http://www.sciencedirect.com/science/article/pii/S0012821X12001628, 2012.

Shepherd, A., Ivins, E. R., A, G., Barletta, V. R., Bentley, M. J., Bettadpur, S., Briggs, K. H., Bromwich, D. H., Forsberg, R., Galin, N., Horwath, M., Jacobs, S., Joughin, I., King, M. A., Lenaerts, J. T. M., Li, J., Ligtenberg, S. R. M., Luckman, A., Luthcke, S. B., McMillan, M., Meister, R., Milne, G., Mouginot, J., Muir, A., Nicolas, J. P., Paden, J., Payne, A. J., Pritchard, H., Rignot, E., Rott, H., Sohn, H.-G.rensen, L. S., Scambos, T. A., Scheuchl, B., Schrama, E. J. O., Smith, B., Sundal, A. V., van Angelen, J. H., van de Berg, W. J., van den Broeke, M. R., Vaughan, D. G., Velicogna, I., Wahr, J., Whitehouse, P. L., Wingham, D. J., Yi, D., Young, D., and Zwally, H. J.: A Reconciled Estimate of Ice-Sheet Mass Balance, Science, 338, 1183–1189, doi:10.1126/science.1228102, http://www.sciencemag.org/content/338/6111/1183.abstract, 2012.

Shimada, R., Takeuchi, N., and Aoki, T.: Inter-annual and geographical variations in the extent of bare ice and dark ice on the Greenland ice sheet derived from MODIS satellite images, Frontiers in Earth Science, 4, doi:10.3389/feart.2016.00043, http://www.frontiersin.org/cryospheric_sciences/10.3389/feart.2016.00043/abstract, 2016.

Stibal, M., Sabacka, M., and Zarsky, J.: Biological processes on glacier and ice sheet surfaces, Nature Geoscience, 5, 771–774, doi:10.1038/ngeo1611, 2012.

Stibal, M., Gozdereliler, E., Cameron, K., Box, J. E., Stevens, I., Gokul, J., Schostag, M., Zarsky, J., Edwards, A., Irvine-Fynn, T., and Jacobsen, C.: Microbial abundance in surface ice on the Greenland Ice Sheet, Frontiers in Microbiology, 6, 225, 2015.

Stroeve, J., Box, J. E., Wang, Z., Schaaf, C., and Barrett, A.: Re-evaluation of MODIS MCD43 Greenland albedo accuracy and trends, Remote Sensing of Environment, 138, 199 – 214, doi:http://dx.doi.org/10.1016/j.rse.2013.07.023, http://www.sciencedirect.com/science/article/pii/S0034425713002356, 2013.

Takeuchi, N., Kohshima, S., and Seko, K.: Structure, Formation, and Darkening Process of Albedo-Reducing Material (Cryoconite) on a Himalayan Glacier: A Granular Algal Mat Growing on the Glacier, Arctic, Antarctic, and Alpine Research, 33, 115–122, http://www.jstor.org/stable/1552211, 2001.

Tedesco, M., Doherty, S., Fettweis, X., Alexander, P., Jeyaratnam, J., Noble, E., and Stroeve, J.: The darkening of the Greenland ice sheet: trends, drivers and projections (1981-2100), The Cryosphere, 10, 477–496, doi:10.5194/tc-10-477-2016, http://www.the-cryosphere.net/10/477/2016/, 2016.

Teeling, H., Fuchs, B. M., Benke, C. M., Krüger, K., Chafee, M., Kappelman, L., Reintjes, G., Waldmann, J., Quast, C., Glöckner, F. O., Lucas, J., Wichels, A., Gerdts, G., Wiltshire, K. H., and Amann, R. I.: Recurring patterns in bacterioplankton dynamics during coastal spring algae blooms, eLife, 5, e11 888, 2016.

Uetake, J., Naganuma, T., Hebsgaard, M. B., Kanda, H., and Kohshima, S.: Communities of algae and cyanobacteria on glaciers in west Greenland, Polar Science, 4, 71 – 80, doi:http://dx.doi.org/10.1016/j.polar.2010.03.002, http://www.sciencedirect.com/science/article/pii/S1873965210000101, 2010.

van As, D., Fausto, R. S., Cappelen, J., van de Wal, R. S. W., Braithwaite, R. J., Machguth, H., and the PROMICE project team: Placing Greenland ice sheet ablation measurements in a multi-decadal context, Geologic Survey of Denmark and Greenland Bulletin, 35, 71–74, 2016.

van den Broeke, M. R., Smeets, C. J. P. P., and van de Wal, R. S. W.: The seasonal cycle and interannual variability of surface energy balance and melt in the ablation zone of the west Greenland ice sheet, Cryosphere, 5, 377–390, doi:10.5194/tc-5-377-2011, http://www.the-cryosphere.net/5/377/2011/, 2011.

van den Broeke, M. R., Enderlin, E. M., Howat, I. M., Kuipers Munneke, P., Noël, B. P. Y., van de Berg, W. J., van Meijgaard, E., and Wouters, B.: On the recent contribution of the Greenland ice sheet to sea level change, The Cryosphere, 10, 1933–1946, doi:10.5194/tc-10-1933-2016, http://www.the-cryosphere.net/10/1933/2016/, 2016.

Warren, S. and Wiscombe, W.: Dirty snow after nuclear war, Nature, 313, 467–470, 1985.

Warren, S. G.: Impurities in snow: effects on albedo and snowmelt, Annals of Glaciology, 5, 177–179, 1984.

Warren, S. G.: Can black carbon in snow be detected by remote sensing?, Journal of Geophysical Research: Atmospheres, 118, 779–786, doi:10.1029/2012JD018476, http://dx.doi.org/10.1029/2012JD018476, 2013.

Warren, S. G. and Wiscombe, W. J.: A model for the spectral albedo of snow. II: Snow containing atmospheric aerosols, Journal of the Atmospheric Sciences, 37, 2734–2745, 1980.

Webster-Brown, J., Hawes, I., Jungblut, A., Wood, S., and Christenson, H.: The effects of entombment on water chemistry and bacterial assemblages in closed cryoconite holes on Antarctic glaciers, FEMS Microbiology Ecology, 91, fiv144, 2015.

Wharton, R. A., McKay, C. P., Simmons, G. M., and Parker, B. C.: Cryoconite Holes on Glaciers, BioScience, 35, 499–503, http://www.jstor.org/stable/1309818, 1985.

Wientjes, I., De Van Wal, R., Schwikowski, M., Zapf, A., Fahrni, S., and Wacker, L.: Carbonaceous particles reveal that Late Holocene dust causes the dark region in the western ablation zone of the Greenland ice sheet, Journal of Glaciology, 58, 787–794, doi:doi:10.3189/2012JoG11J165, http://www.ingentaconnect.com/content/igsoc/jog/2012/00000058/00000210/art00016, 2012.

Wientjes, I. G. M. and Oerlemans, J.: An explanation for the dark region in the western melt zone of the Greenland ice sheet, The Cryosphere, 4, 261–268, doi:10.5194/tc-4-261-2010, http://www.the-cryosphere.net/4/261/2010/, 2010.

Yallop, M. L., Anesio, A. M., Perkins, R. G., Cook, J., Telling, J., Fagan, D., MacFarlane, J., Stibal, M., Barker, G., Bellas, C., Hodson, A., Tranter, M., Wadham, J., and Roberts, N.: Photophysiology and albedo-changing potential of the ice algal community on the surface of the Greenland ice sheet, The ISME Journal, 6, 2302–2313, doi:10.1038/ismej.2012.107, 2012.